University of São Paulo
Luiz de Queiroz College of Agriculture

Weathering and incipient pedogenesis of Technosols constructed from dolomitic limestone mine spoils

Francisco Ruiz

Dissertation presented to obtain the degree of Master in Science. Area: Soil and Plant Nutrition

Piracicaba
2019

Francisco Ruiz
Agronomist

Weathering and incipient pedogenesis of Technosols constructed from dolomitic limestone mine spoils

versão revisada de acordo com a resolução CoPGr 6018 de 2011

Advisor:
Prof. Dr. **TIAGO OSÓRIO FERREIRA**

Dissertation presented to obtain the degree of Master in Science. Area: Soil and Plant Nutrition

Piracicaba
2019

Dados Internacionais de Catalogação na Publicação
DIVISÃO DE BIBLIOTECA – DIBD/ESALQ/USP

Ruiz, Francisco

Weathering and incipient pedogenesis of Technosols constructed from dolomitic limestone mine spoils / Francisco Ruiz. - - versão revisada de acordo com a resolução CoPGr 6018 de 2011. - - Piracicaba, 2019.

74 p.

Dissertação (Mestrado) - - USP / Escola Superior de Agricultura "Luiz de Queiroz".

1. Solos tecnogênicos 2. Processos pedogenéticos 3. Morfologia de solos 4. Alteração mineral 5. Rizosfera I. Título

AGRADECIMENTOS

O maior dos agradecimentos é destinado a meus pais, Domingos e Nádia, pelo amor e apoio incondicionais durante todos os anos de minha vida, sem os quais este trabalho não seria realizado, de forma alguma.

Agradeço ao professor e orientador Tiago O. Ferreira pela confiança, pelo aprendizado e por todo suporte para contornar os obstáculos até aqui.

A todos da equipe GepGeoq, Gabriel, Danilo, Daniel, Hermano, Glêvia, Fábio, Verônica, Laís, Isadora, Thayana, Geraldo e Diego, por toda ajuda e amizade, especialmente a Douglas e Beatriz, pelos trabalhos de campo e laboratório.

A Lucas Sartor, pelo grande apoio e forte amizade desde os primórdios da minha iniciação científica. Também gostaria de destacar o agradecimento a Leandro Goia pela amizade e por todo suporte em campo e laboratório.

Aos professores Jean e Valdomiro, da UFRPE, por toda contribuição a este trabalho. A Arnaldo Souza e ao prof. José Alexandre Melo Demattê, da ESALQ-USP, também pelas contribuições.

Obrigado a todos os amigos da melhor república do universo, GMR Xapadão, minha segunda família.

À Tainá Patriani sou imensamente grato pela companhia incrível, pelo amor e pelo importantíssimo apoio emocional.

À mineradora Calcário Amaral Machado pela concessão da área de estudo.

Por fim, gostaria de agradecer à Coordenação de Aperfeiçoamento de Pessoal de Nível Superior (CAPES) pelo suporte financeiro.

SUMMARY

RESUMO

Intemperismo e pedogênese incipiente em Tecnossolos desenvolvidos a partir de rejeitos de mineração de calcário dolomítico

Tecnossolos são uma classe de solos cuja pedogênese é dominada por sua origem antrópica. Esses solos contêm uma quantidade significativa de materiais feitos, modificados ou transportados diretamente pela atividade humana, definidos como artefatos. Solos formados a partir de materiais de origem antrópicos são muito comuns, entretanto sua pedogênese ainda é pouco compreendida. O uso sustentável do recurso solo exige um amplo conhecimento sobre sua gênese, sendo assim, entender a formação de Tecnossolos, especialmente no ambiente tropicalé crucial para seu uso e manejo visando sua incorporação na produçao de alimento, fibras e energia. Neste estudo foram estudados três Tecnossolos construídos a partir de rejeitos de mineração de calcário dolomítico, cultivados por dois e seis anos com cana-de-acúcar e por 20 anos sob pastagem. Os Tecnossolos apresentaram uma rápida evolução morfológica expressa principalmente pelo desenvolvimento de cor e agregação. Dentre os processos identificados, os mais importantes foram pedoplasmação, melanização e os redoximórficos. Devido à combinação de gramíneas e rejeitos ricos em cálcio desenvolveu-se um horizonte de superfície com estrutura grumosa forte e cor escura, com altos teores de carbono orgânico. A rizosfera desempenhou um papel fundamental no intemperismo mineral dos Tecnossolos. A exsudação e a atividade microbiana foram cerca de duas vezes maiores na rizosfera do que no solo não rizosférico, levando a uma dissolução mineral mais proeminente na rizosfera. No geral, os minerais primários da rizosfera apresentaram um grau médio/alto de intemperismo, enquanto aqueles do solo não rizosférico foram pouco intemperizados. As condições biogeoquímicas da rizosfera apontam para um ambiente favorável à formação de minerais de argila na rizosfera. O estudo demonstra que a pedogênese de Tecnossolos emambiente tropical parece avançar rapidamente; o que pode garantir não só o sucesso da reabilitação das áreas, mas ainda a retomada de serviços ecossistêmicos prestados pelos solos.

Palavras-chave: Solos tecnogênicos; Processos pedogenéticos; Morfologia de solos; Alteração mineral; Rizosfera

ABSTRACT

Weathering and incipient pedogenesis of Technosols constructed from dolomitic limestone mine spoils

Technosols combine soils subjected to strong human influence and whose pedogenesis is dominated by its technical origin. They contain a significant amount of materials made, modified or directly transported by human activity, defined as artefacts. Soils formed from technogenic parent materials are spreading and their pedogenesis is still little understood. Given that the sustainable use of the soil resources demands wide knowledge about its genesis, it is necessary to bring further information about Technosols, especially in the tropical environment, where they have been poorly explored. Thus, in this study we characterized three Technosols constructed from dolomitic limestone mine spoils, cultivated with sugar cane (for 2 and 6 years) and pasture (for 20 years). The Technosols experienced a rapid morphological evolution expressed by color development and aggregation. Pedoplasmation, melanization and redoximorphic were the mainly processes occurring in these constructed soils. The combination of grasses over Ca-rich mine spoils triggered organic carbon accumulation and originated a well-developed surface horizon with strong crumb structure and dark color. The rhizosphere played a pivotal role in mineral weathering of the Technosols. Exudation and microbial activity were about two times higher in the rhizosphere than in the bulk soil leading to an enhanced mineral dissolution. Overall, the primary minerals in the rhizosphere presented a medium to high degree of weathering while those from bulk soil were little weathered. Our data indicates that the rhizosphere may provide a favorable biogeochemical environment to the formation of secondary clay minerals. This study evidences that constructed tropical soils may evolve in an accelerated rate of pedogenesis and, thus, are a real alternative for the reclamation of degraded areas, potentially restoring original soil ecosystem services.

Keywords: Technogenic soils; Pedogenetic processes; Soil morphology; Mineral alteration; Rhizosphere

1. INTRODUCTION

Anthropogenic soils are those whose pedogenetic processes are originated, modified or derived from anthropic activities (Certini and Scalenghe, 2011). In most locations, humans have modified, reorganized, or transported soils and/or soil materials, thus these soils are distributed throughout the planet, occurring mainly in urban, agricultural and mining areas (Capra et al., 2015). In 2006, anthropogenic soils were recognized by the World Reference Base for Soil Resources (WRB-FAO) and constituted the Anthrosols and Technosols groups (IUSS Working Group WRB, 2006). The first group comprises soils resulting from a long-term human activity with the addition of organic and inorganic materials, developing anthropic horizons, e.g. plaggic, hortic, pretic (Bulgariu et al., 2012; Giani et al., 2014; Macedo et al., 2017). Technosols, on the other hand, are essentially developed on materials made, modified or exposed by human activity that otherwise would not occur at the Earth's surface, known as artefacts (IUSS Working Group WRB, 2014). Taxonomically, a Technosol has a technic hard material within 5 cm or a geomembrane or a significant amount of artefacts (>20% by volume) within 100 cm. Its pedogenesis is thus inherent to the type and organization of these materials in the soil (IUSS WORKING GROUP WRB, 2006). Technosols are often referred as urban, mining or technogenic soils (Rosembaum et al., 2003)

The diversity of technogenic materials (artefacts) includes waste from industrial, mining and urban activities, such as household wastes, construction debris, sludge, ashes and mine spoils (Huot et al., 2014; Pellegrini et al., 2016; Vidal-Beaudet et al., 2018; Villenave et al., 2018). The chemical and physical characteristics of these materials may differ from those usually found in rocks and sediments that give rise to natural soils. Due to the recent exposure of anthropic materials, Technosols may present little pedogenetic development (Leguédois et al., 2016). However, recent studies have evidenced that the action of pedogeneticprocesses and genesis of the morphologicalcharacteristics are often similar to those observed in "natural soils". Studies conducted in Europe (Huot et al., 2013), have found pseudo-allophane minerals formation through the alteration of iron and manganese oxides from iron industry tailings. Other studies on constructed soils evidenced the formation of anthropic surface horizons, with the development of soil peds in a small-time frame (<5 years) of pedogenesis (Scalenghe and Ferraris, 2009; Séré et al., 2010).

Considering the rapid growth of the world´s population and the association of these soils with human activity, anthropogenic soils gained great environmental, economic, social and cultural importance. It is estimated that 70% of the globalpopulation will be living in urban centers by 2050 (Morel et al., 2014) and, therefore, it is expected that the increasing urbanization will be accompanied by transformations of the natural landscape. As a result, human-made soils will be more frequent. Understanding their pedogenetic processes (type and intensity) will ensure a better knowledge on its functioning supporting proper management and sustainable use. In other words, understanding soil genesis of these young artificial soils is pivotal to recognize their potential to generate energy, food and fibers, providing ecosystem services and, thus, optimizing land reclamation.

Studies of Technosols on tropical environments are scarce. The first specific publications on Technosols date back to 2009. Until 2018, 31 papers were published on pedogenesis of Technosols; five of those in tropical environments but none in Brazil (Scopus base, 2018). Although the international soil classification systems such as the World Reference Base (IUSS WORKING GROUP WRB, 2014) and Soil Taxonomy (Soil Survey Staff, 2014) contemplate anthropogenic soils, the current Brazilian Soil Classification System (SiBCS, Embrapa, 2018) does not recognize these soils as a specific soil order. Studies on pedogenesis of anthropogenic soils may highlight their importance and contribute to the updating of SiBCS.

Among the anthropic activities, mining stands out as one of the most harmful to natural landscapes causing large-scale ecosystem degradation (Lima et al., 2016). Soil and water pollution, erosion and deforestation are among some of the impacts caused by mining operations (Robles-Arenas et al., 2006; Swenson et al., 2011; Thornton et al., 2006). In surface mining the entire regolith and the overlying rocks are removed for ore exploration, producing deep open-pits. The removal of topsoil and its deposition with the overburden generate large piles of mine spoils. Consequently, this activity produces cut-and-fill landforms of various types and produces degraded landscapes unlikely for natural regeneration (Szabó, 2010).

It is estimated that in the period from 2010 to 2030, more than 11 billion tons of mining tailings will be generated in Brazil (IPEA, 2012). São Paulo State, Brazil, comprise an important dolomitic limestone mining center with more than 4 million tons (DNPM, 2000) where limestone mining is carried out in open-pits. Particulary in Saltinho municipality (Irati Formation; Assistência member) the limestone layers are intercalated with organic black shale and black non-bituminous shales (IPT, 1981) which, as the overlying rocks, are not exploited. These mine spoils include the topsoil, rock fragments (i.e., silex cobbles, siltstones, shales) and impure limestones. The amount of waste generated is often abandoned in large piles exceeding in 13 times (mass base) that of the exploited ore (Souza, 2003). It is evident, therefore, the importance of a correct disposal in order to minimize environmental impacts. In this context, as an effort to minimize mining impacts and aiming to rehabilitate the degraded landscapes, a limestone mining company fulfilled exhausted pits using mine spoils and destined these areas to agriculture.

The present work studied the morphology, biogeochemical and mineralogical data of three Technosols constructed from dolomitic limestone mine spoils and cultivated with tropical grasses (sugar cane and pasture). As an initial approach to technogenic soil formation in tropical environment, we assessed the mineral alterations and pedogenetic evolution occurring in these soils.

References

Bulgariu, D., Feodor, F., Rusu, C., Bulgariu, L., 2012. PEDOGEOCHEMISTRY OF HORTIC ANTHROSOL FROM COPOU GREENHOUSE – IASI (II), Scientific papers, Agronomy Series.

Capra, G.F., Ganga, A., Grilli, E., Vacca, S., Buondonno, A., 2015. A review on anthropogenic soils from a worldwide perspective. https://doi.org/10.1007/s11368-015-1110-x

Certini, G., Scalenghe, R., 2012. Anthropogenic soils are the golden spikes for the Anthropocene, The Holocene. https://doi.org/10.1177/0959683611408454

DNPM- Departamento nacional de produção mineral, 2000. Anuário Mineral Brasileiro.

EMBRAPA - Empresa brasileira de pesquisa agropecuária 2018. Sistema brasileiro de classificação de solos. 5 ed. Brasília,

Giani, L., Makowsky, L., Mueller, K., 2014. Plaggic Anthrosol: Soil of the Year 2013 in Germany: An overview on its formation, distribution, classification, soil function and threats.J.PlantNutr. Soil Sci. 177, 320–329. https://doi.org/10.1002/jpln.201300197

Huot, H., Faure, P., Biache, C., Lorgeoux, C., Simonnot, M.-O., Morel, J.L., 2014. A Technosol as archives of organic matter related to past industrial activities. Sci. Total Environ. 487, 389–398. https://doi.org/https://doi.org/10.1016/j.scitotenv.2014.04.047

Huot, H., Simonnot, M.-O., Marion, P., Yvon, J., Donato, P., Morel, J.-L., 2013. Characteristics and potential pedogenetic processes of a Technosol developing on iron industry deposits. J. Soils Sediments 13, 555–568. https://doi.org/10.1007/s11368-012-0513-1

IPEA -Instituto de pesquisa aplicada, 2012. Diagnóstico dos Resíduos Sólidos da Atividade de Mineração de Substâncias Não Energéticas. Plano Nacional de Resíduos Sólidos.

IPT - INSTITUTO DE PESQUISAS TECNOLÓGICAS DO ESTADO DE SÃO PAULO, 1981b. Mapa Geológico do Estado de São Paulo - escala 1:500.000. Divisão de Minas e Geologia Aplicada. 2v. (IPT, Série Monografias, 6).

IUSS Working Group WRB, 2006. World reference base for soil resources 2014. International soil classification system for naming soils and creating legends for soil maps, World Soil Resources Reports No. 103.

IUSS Working Group WRB, 2014. World reference base for soil resources 2014. International soil classification system for naming soils and creating legends for soil maps, World Soil Resources Reports No. 106. https://doi.org/10.1017/S0014479706394902

Leguédois, S., Séré, G., Auclerc, A., Cortet, J., Huot, H., Ouvrard, S., Watteau, F., Schwartz, C., Morel, J.L., 2016. Modelling pedogenesis of Technosols. Geoderma 262, 199 –212. https://doi.org/10.1016/j.geoderma.2015.08.008

Lima, A.T., Mitchell, K., O'Connell, D.W., Verhoeven, J., Van Cappellen, P., 2016. The legacy of surface mining: Remediation, restoration, reclamation and rehabilitation. Environ. Sci. Policy 66, 227–233. https://doi.org/https://doi.org/10.1016/j.envsci.2016.07.011

Macedo, R.S., Teixeira, W.G., Corrêa, M.M., Martins, G.C., Vidal-Torrado, P., 2017. Pedogenetic processes in anthrosols with pretic horizon (Amazonian Dark Earth) in Central Amazon, Brazil. PLoS One 12, e0178038.

Morel, J.L., Chenu, C., Lorenz, K., 2014. Ecosystem services provided by soils of urban , industrial , traffic , mining , and military areas (SUITMAs). https://doi.org/10.1007/s11368-014-0926-0

Pellegrini, S., García, G., Peñas-Castejon, J.M., Vignozzi, N., Costantini, E.A.C., 2016. Pedogenesis in mine tails affects macroporosity, hydrological properties, and pollutant flow. Catena 136, 3–16. https://doi.org/10.1016/j.catena.2015.07.027

Robles-Arenas, V.M., Rodríguez, R., García, C., Manteca, J.I., Candela, L., 2006. Sulphide-mining impacts in the physical environment: Sierra de Cartagena–La Unión (SE Spain) case study. Environ. Geol. 51, 47–64. https://doi.org/10.1007/s00254-006-0303-4

Rosenbaum, M.S., McMillan, A.A., Powell, J.H., Cooper, A.H., Culshaw, M.G., Northmore, K.J., 2003. Classification of artificial (man-made) ground. Eng. Geol. 69, 399–409. https://doi.org/10.1016/S0013-7952(02)00282-X

Rossiter, D.G., 2007. Classification of urban and industrial soils in the World Reference Base for Soil Resources. J. Soils Sediments 7, 96–100. https://doi.org/10.1065/jss2007.02.208

Scalenghe, R., Ferraris, S., 2009. The First Forty Years of a Technosol. Pedosphere 19, 40–52. https://doi.org/10.1016/S1002-0160(08)60082-X

Séré, G., Schwartz, C., Ouvrard, S., Renat, J.C., Watteau, F., Villemin, G., Morel, J.L., 2010. Early pedogenic evolution of constructed Technosols. J. Soils Sediments 10, 1246–1254. https://doi.org/10.1007/s11368-010-0206-6

Soil Survey Staff. 2014. Keys to Soil Taxonomy, 12th ed. USDA-Natural Resources Conservation Service, Washington, DC.

Souza, M. H. O., 2003. Separação do calcario e do folhelo pirobetuminoso da formação Irati para a utilização como corretivo e como aditivo na indústria cerâmica. Thesis (Doctorate degree in Geosciences) UNESP- Rio Claro,

Swenson, J.J., Carter, C.E., Domec, J.-C., Delgado, C.I., 2011. Gold Mining in the Peruvian Amazon: Global Prices, Deforestation, and Mercury Imports. PLoS One 6, e18875.

Szabó, J., 2010. Anthropogenic Geomorphology: Subject and System BT - Anthropogenic Geomorphology: A Guide to Man-Made Landforms, in: Szabó, J., Dávid, L., Lóczy, D. (Eds.), . Springer Netherlands, Dordrecht, pp. 3–10. https://doi.org/10.1007/978-90-481-3058-0_1

Thornton, E.B., Sallenger, A., Sesto, J.C., Egley, L., McGee, T., Parsons, R., 2006. Sand mining impacts on long-term dune erosion in southern Monterey Bay. Mar. Geol. 229, 45 –58. https://doi.org/https://doi.org/10.1016/j.margeo.2006.02.005

Vidal-Beaudet, L., Rokia, S., Nehls, T., Schwartz, C., 2018. Aggregation and availability of phosphorus in a Technosol constructed from urban wastes. J. Soils Sediments 18, 456–466. https://doi.org/10.1007/s11368-016-1469-3

Villenave, C., Séré, G., Schwartz, C., Watteau, F., Jimenez, A., Cortet, J., 2018. Rapid Changes in Soil Nematodes in the First Years after Technosol Construction for the Remediation of an Industrial Wasteland. Eurasian Soil Sci. 51, 1266–1273. https://doi.org/10.1134/S1064229318100149

2. MORPHOLOGICAL EVOLUTION AND PEDOGENETIC PROCESSES OF TECHNOSOLS DEVELOPED FROM DOLOMITIC LIMESTONE MINE SPOILS

Abstract

Technosols are found wherever human activity has led to the construction of artificial soils. Mine spoils, for example, are common parent materials in Technosols. In this study, we characterized three constructed soil profiles developed from dolomitic limestone mine spoils, where sugarcane has grown for two (SC2) and for six years (SC6) and pasture has grown for 20 years (P20). Routine chemical and physical analyses as well as macro and micromorphological investigations were conducted. An advanced stage of pedoplasmation led to further aggregation when comparing SC2 and SC6 profiles. Dissolution of iron nodules is an important mechanism of matrix pigmentation in SC6 and pyrite oxidation also seems to contribute, especially in subsurface. Redoximorphic features are present in SC6 subsurface because of temporary waterlogging conditions. In P20 the mainly pedogenetic process occurring is melanization. The high amount of organic carbon (>7.4%) is partially explained by the abundant addition of fresh organic matter via roots death, which enhanced humification rates. High exchangeable calcium content mediated stabilization of organic matter. A strong crumb structure and dark matrix color appear at surface horizons consequently. Our results evidence the intensity and the concomitance of different pedogenetic processes and the rapid morphological evolution of these Technosols in a time scale of only 20 years.

Keywords: Constructed soils; Soil genesis; Micromorphology; Mine reclamation; Tropical grasses

2.1. Introduction

Technosol is a soil order, recognized by the World Reference Base for Soil Resources (WRB-FAO) since 2006, andcharacterized by the significant amount (> 20% in volume) of technogenic material. Mine spoils are artefacts (any material created, transported or modified by human activity) and common parent material for Technosols (IUSS Working Group WRB, 2014). The many ways technogenic materials of mine sites can be modified include blasting and excavation of bedrock, transportation, crushing and mixing (Szabó, 2010), which may strongly determine the kinetics of weathering and, thus, control soil formation (Duchaufour, 1982).

Besides influencing parent materials, humans also interfere with other soil forming factors in Technosols. For example, organisms can be modified by replacement of natural forest by domesticated plants, or by selecting specific species for land remediation/rehabilitation (Howard, 2017; Lima et al., 2016). The establishment of plants over anthropic material can promote significant action in Technosol weathering.

It has been observed that in few years plants induce accelerated structure evolution in Technosols by promoting aggregation, via addition of organic matter and roots activity (Huot et al., 2014; Jangorzo et al., 2013). Moreover, vegetation can cause specific soil processes (e.g. podzolization, melanization) that defines soil morphology and profile evolution (Pawlik and Šamonil, 2018).

To fulfill basic soil functions and allow plant installation and growth, mine land reclamation usually relies on constructed Technosol as an important part of the process. In some cases, amendments are required to improve soil attributes, e.g. increase in cation exchange capacity and nutrients availability, water retention and immobilization of heavy metals (Asensio et al., 2015; Rodríguez-Vila et al., 2017, 2015). There are situations, however, where technogenic soils are developed directly from mine spoils (Sokolov et al., 2015), excavated bedrock and sediments (Scholtus et al., 2015). When physical-chemical properties of the technogenic material are favorable, vegetation can develop directly from these technogenic materials (Séré et al., 2010).

In the city of Saltinho (SE- Brazil, São Paulo State), open-pit mining is carried out to exploit the limestone ore contained in the Irati Formation (Assistência member). In order to rehabilitate the degraded landscape, a limestone mining company, Calcário Amaral Machado, constructed Technosols by fulfilling three exploited open casts using the mine spoils. Then, these areas were aimed to agriculture (sugar cane, for 2 and 6 years and pasture, for 20 years), exploring the plant growth potential they could provide. Since then, pedogenesis enhanced by tropical grasses activity is taking place in these young soils.

Assuming that the combination of tropical climate and intense plant activity may drive to fast pedogenesis in Technosols developed from limestone mining spoils, we expected to verify significant profile development when comparing the three Technosols (sugar cane 2 years, sugar cane 6 years and pasture 20 years). For this, we aimed to assess the macro and micromorphological evolution of three constructed Technosols, seeking to identify the main pedogenetic processes in hese human-made soils.

2.2. Materials and methods

2.2.1. Description of the study area

The study was conducted in an operating limestone mine in Southeast Brazil (São Paulo state, Saltinho municipality) (Fig. 1). The regional climate, according to Koeppen classification system, is humid subtropical (Cwa), with average annual temperature of 21.4ºC, annual rainfall of 1213 mm, most concentrated between November and March (CEPAGRI, 2018). The natural vegetation consists of semi-evergreen forest (IBGE, 2012). The study area is over the transitioning of the Assistência Member of the Irati Formation and the Corumbataí Formation. The local lithology is dominated by the presence of dolomites, partially dolomitized limestones, black shales and silex nodules from the Assistência Member (Irati Formation); and gray siltstones from the Corumbataí Formation.

The mining company rehabilitated three former open-casts by fulfilling it with the limestones mine spoils. These areas were composed mostly by siltstones and black shales that were exploded, excavated and mixed, generating fragments of varied granulometry. After reshaping the topography with the mine spoils, the newly constructed soils were destined to agriculture. Sugar cane has grown in two areas, one for 2 years and the other for 6 years (SC2 and SC6, respectively), while a *Brachiaria spp* pasture of 20 years old (P20) was established in the last one (Fig.1).

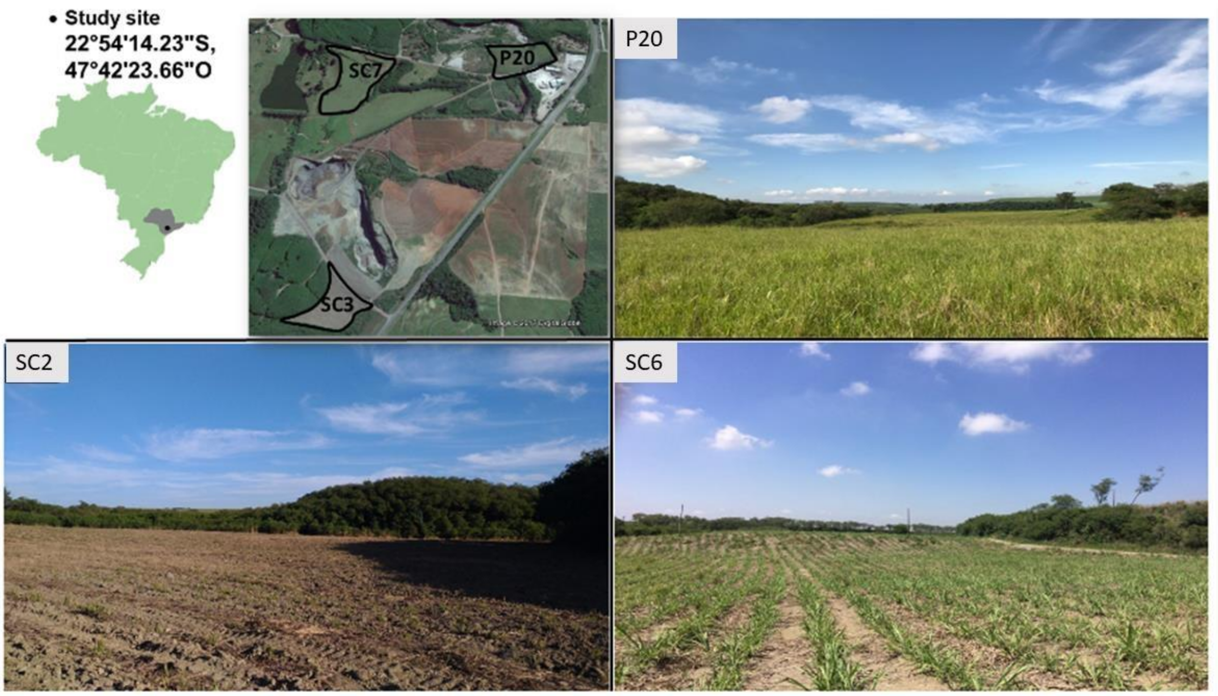

Fig.1 Location of the mining company and distribution of the rehabilitated open-pits in Saltinho city, State of São Paulo, Brazil. Photographs of the 2 years old sugar cane area (SC2), 6 years old sugar cane area (SC6) and 20 years old pasture (P20).

2.2.2. Soil description, sampling and analyzing

A soil pit was dug in each one of the areas for soil sampling and profile description. The macromorphological features were described according to the Guidelines for Soil Description (Jahn et al., 2006) and the profiles were classified according to the World Reference Base (IUSS Working Group WRB, 2014). For physical and chemical characterization, samples were collected from each horizon of the soil profiles. The samples were dried at 40º C for 72 h and sieved (< 2 mm for chemical analysis and < 0,025mm for carbon determination). The percentages of coarse and fine fraction were sieved and their volume estimated using a 1000 mL graduated cylinder. Granulometric analysis was carried out on the fine earth after treatment with H_2O_2 to remove organic matter. The sand was separated using a 0,053mm sieve and the clay was separated from the silt fraction by sedimentation (Stoke's law) in an alkaline suspension containing sodium hexametaphosphate (Gee and Or, 2002).

The pH was determined with a pH electrode in deionized water (soil: solution ratio, 1:2,5). Exchangeable K^+, Na^+ and available P were extracted with acidic Mehlich 1 solution. The K and Na contents were determined by flame spectroscopy (Digimed DM-62) and P by spectrophotometry, while exchangeable Ca2+ and Mg2+ were extracted with KCl 1.0 mol L-1 solution and determined by atomic absorption spectroscopy (Perkin Elmer 1100B). Potential acidity (H+Al) was measured by titration of the solution with NaOH after extraction with calcium acetate at pH 7.0. Carbon contents were measured in an elemental analyzer (SSM-5000A) and the total inorganic carbon (TIC) was calculated as the difference between total soil carbon and total organic carbon (TOC), after the removal of inorganic carbon with 3 mol L^{-1} HCl solution (Soil Survey Staff, 2011).

2.2.3. Micromorphology and scanning electron microscopy (SEM) with electron dispersive x-rays (EDS)

Undisturbed 0-10 cm blocks were collected from the three soil profiles (additionally, a 50-60cm block was collected from SC6) for the preparation of the thin sections. The samples were oven-dried at 40ºC for 72h. Impregnation, sawing and grinding were carried out according to Murphy (1987). Description was made following guidelines recommended by Bullock et al. (1985) and Stoops et al. (2010), including the assessment of mineral and organic phases, microstructure and pedo-features. The thin sections were also subjected to Scanning Electron Microscopy with Energy Dispersive Spectroscopy (SEM-EDS) in order to achieve more details of pedo-features.

2.3. Results

2.3.1. Physico-chemical attributes, soil morphology and classification

Soil profiles are shown in Fig. 2 and morphological data can be visualized in Table 1 (see Annexes for details). The three soil profiles were classified as Hyperskeletic Spolic Technosol, with changes in the supplementary qualifiers: SC2 is Clayic, SC6 is Clayic, Endoraptic, and P20 is Hyperumic, Loamic, Somerimollic. The primary qualifiers indicate that the three profiles contain >35% of mine spoils as artefacts and have <20% fine earth. The "Endoraptic" qualifier in SC6 indicates lithological discontinuity in 2Chu3 horizon where the composition of the mine spoils abruptly changes from abundant siltstones and very few black shales to dominant black shales. P20 acquired "somerimollic" and "hyperhumic" qualifiers due to the presence of a mollic epipedon <20cm thick and containing >5% soil organic carbon to a depth of 50cm, respectively.

SC2 presented weak fine granular structure in the ACu horizon (0-7cm) and very weak fine granular in the CAu horizon, both with dark grayish brown matrix color. The subjacent horizons were composed mostly by coarser fractions of siltstone gravels and stones and rare black shale fragments with single grain structure. Some siltstones exhibit initial stage of alteration. Very few reddish yellow mottles were observed along the profile and roots were concentrated mainly in the ACu horizon.

A thicker (0-9cm) dark grayish brown (10YR 4/1) ACu horizon with reddish yellow (7.5 YR 6/8) and red mottles (2.5 YR 4/8) is observed in the SC6 profile, exhibiting weak to moderated fine and medium granular structure and weak fine subangular blocky structure. CAu and C1u presented less developed structures than ACu, with the latter having larger amounts of coarse material and single grain structure. Siltstones fragments are strongly altered. The Cgu2 is shown with reddish yellow matrix color (7.5 YR 6/8), dark gray (10YR 4/1) and red mottles (2.5 YR 4/8) and the structure is weak fine granular and weak medium subangular blocky. The boundary to the bottom 2Chu3 horizon is abrupt, where black shale fragments predominate as parent material. In this horizon the matrix color is very dark gray (10YR 2/1) with few reddish yellow mottles (7.5 YR 6/8), the structure is weak fine granular and TOC, pH and P values increase with respect to the overlying horizons. An indurated layer composed by very large black shale boulders underlies 2Chu3 horizon.

P20 showed a more developed soil structure. Strong crumb and moderate to strong subangular blocky structures appear in Ahu1 and Ahu2 horizons with the presence of many roots. Mottles are absent and the matrix color is very dark brown (7.5 YR 2.5/2). Black shales predominate over siltstones and there are very few dolomitic limestone gravels. Despite the high carbon content in the profile, especially in the Ahu2 horizon (12.2% TOC), there was no sign of undecomposed organic matter, i.e. O layer, accumulation at the surface.

Chemical results (Table 2) shows that P20 profile presented the highest cation exchange capacity (CEC), 34.8 ± 2.0 cmolc kg^{-1}, TOC, 8.23 ± 1.75%, and TIC values, 0.88 ± 0.32% (mean values). The Ca^{2+} content and the base saturation (BS) values are higher in this profile as well. In SC6 we observed the lowest pH values, especially in the ACu and Cug2 horizons (6.8 and 6.6) and an increase in TOC content from 0.4% in Cug 2 to 4.6% in 2Chu3 horizon.

Physical data is displayed in Table 3. Gravels are erratically distributed along the studied profiles. Grain size distribution of the fine earth in SC2 and SC6 are similar (clayic), except for 2Chu3 horizon, where the nature of the mine spoil is similar to those at the P20 profile (loamic). Overall, there is an increase of the fine earth fraction towards the surface, especially in P20, where silt and clay content are higher in the upper horizons.

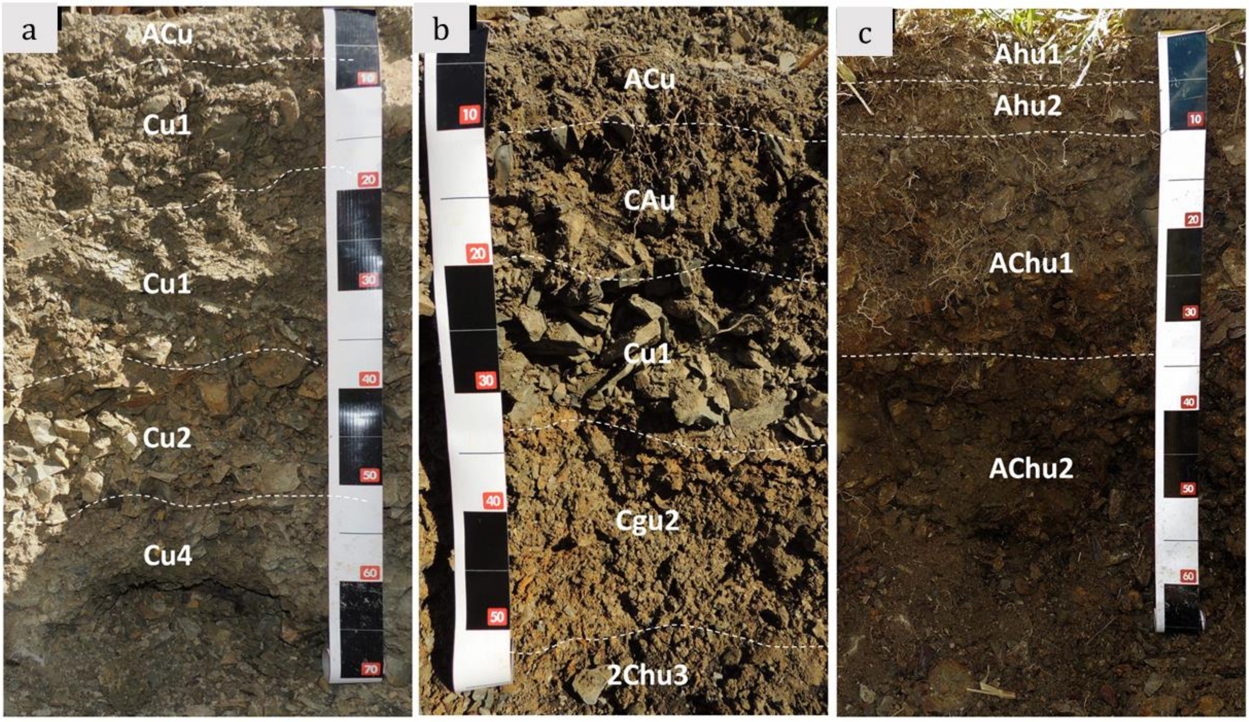

Fig. 2: (a) SC2: Hyperskeletic Spolic Technosol (Clayic); (b) SC6: Hyperskeletic Spolic Technosol (Clayic, Endoraptic); P20: Hyperskeletic Spolic Technosol (Hyperhumic, Loamic, Somerimollic)

Table 1. Macromorphological attributes of SC2, SC6 and P20 soil profiles

Horizon/depth (cm)	Matrix Colour	Mottles		Structure[2]	Consistence[3]	Roots[4]	Artefacts[5]	Boundary[6]
		Color	Quantity. Contrast [1]				type. abundance. size	
SC2: Hyperskeletic Spolic Technosol (Clayic)								
Au (0-7)	10YR 4/1	7.5 YR 6/8	vf. p	w. f. gr	vfr. ss. p	c. fi	ss. a. c; os. vf. c	cl. smo
C1u (7-20)	10YR 4/2	7.5 YR 6/8	vf. p	vw. f. gr	vfr. ss.p	f. fi	ss. d. c; os. vf. c	cl. smo
Cu2 (20-33)	10YR 4/2	7.5 YR 6/8	vf. p	Sgr	ss. p	vf. fi	ss. a. c; os. vf. c	cl. smo
Cu3 (33-52)	10YR 4/2	7.5 YR 6/8	vf. p	Sgr	ss. p	vf. fi	ss. d. c; os. vf. c	cl. smo
Cu4 (52-70+)	10YR 4/2	-	vf. p	Sgr	ss. p	vf. fi	ss. a. c; os. vf. c	
SC6: Hyperskeletic Spolic Technosol (Clayic. Endoraptic)								
Au (0-9)	10YR 4/1	7.5 YR 6/8; 2.5 YR 4/8	a.p; c.p	w/mo. f/m. gr; w.f.sb.	fri. s. p	c. fi	ss. a. c; os. vf. c	cl. smo
CAu (11-21)	10YR 4/2	7.5 YR 6/8; 2.5 YR 4/8	a.p; c.p	w. f. gr	fri. s. p	f.fi	ss. a. c; os. vf. c	cl. smo
Cu1 (21-35)	10YR 4/2	7.5 YR 6/8; 2.5 YR 4/8	c.p; f.p	w. f. gr; sgr	vfri. s. p	f. fi	ss. d. c; os. vf. c	cl. smo
Cgu2 (35-52)	7.5 YR 6/8	10YR 4/1; 2.5 YR 4/8	a.p; f.p; vf. p	w. f. gr; w. m. sb	fri. s. p	f. fi	ss. a. c; os. vf. c	cl. abr
2Chu3 (52-60)	10YR 2/1	7.5 YR 6/8	f. p	w. f. gr	fri. ss. sp	f. fi	os. d. c	
P20: Hyperskeletic Spolic Technosol (Hyperhumic, Loamic, Somerimollic)								
Ahu1 (0-5)	7.5 YR 2.5/2	-	-	st. m/c. cr; mo. m. sb.	firm. ss. sp	m. fi/me	os. a. c; ss. a. c.; do. vf. c.	cl. smo
Ahu2 (5-11)	7.5 YR 2.5/2	-	-	mo/st. m. cr; mo. f. bs	firm. ss. sp	m. fi/me	os. a. c; ss. a. c.; do. vf. c.	cl. smo
AChu1 (11-29)	7.5 YR 2.5/2	-	-	mo. f/m. gr	fri. ss. sp	m. fi/me	os. a. c; ss. a. c.; do. vf. c.	cl. smo
AChu2 (29-60+)	7.5 YR 2.5/2	-	-	mo. f. gr	fri. ss. sp	c. fi	os. d. c.; ss. f. c. do. vf. c.	

1) vf = very few, f = few, c = common, a = abundant; p = prominent
2) vw = very weak, w = weak, mo = moderate, st= strong; f= fine, m= medium; sgr = single grain, gr = granular, cr = crumb, sb= subangular blocky
3) vfr= very friable, fri = friable, firm = firm; ss= slight sticky, s = sticky, sp = slightly plastic, p = plastic
4) vf= very few, c = common, m = many; fi = fine, me = medium
5) ss = siltstone, os = black shale; do: dolomite; vf = very few a = abundant, d = dominant; c= coarse
6) cl= clear, smo= smooth

Table 2. Chemical attributes of SC2, SC6 and P20 soil profiles

Horizon/depth (cm)	pH	TOC %	TIC %	Na^+	K^+	Ca^{2+}	Mg^{2+}	H^++Al^{3+}	P mg kg^{-1}	CEC (pH 7.0) cmolc kg^{-1}	Base sat. %	m
				--cmolc kg^{-1}------------------------------								
SC2: Hyperskeletic Spolic												
ACu (0-7)	7.1	0.7	-	0.2	0.3	10.0	12.5	2.1	129.9	25.1	91.6	<0.1
Cu1 (7-20)	7.2	0.5	-	0.5	0.3	9.8	12.1	2.1	120.1	24.7	91.4	<0.1
Cu2 (20-33)	7.6	0.4	-	0.8	0.2	10.1	15.1	2.1	100.5	28.4	92.5	<0.1
Cu3 (33-52)	7.4	0.4	-	1.1	0.3	10.8	14.9	2.2	178.6	29.2	92.5	<0.1
Cu4 (52-70+)	7.8	0.4	-	1.3	0.3	10.3	13.9	2.0	141.2	27.8	92.8	<0.1
SC6: Hyperskeletic Spolic Technosol (Clayic Endoraptic)												
ACu1 (0-9)	6.8	0.8	-	0.2	0.3	11.2	14.3	2.5	18.1	28.5	91.3	<0.1
CAu (11-21)	6.9	0.5	-	0.2	0.2	11.6	11.2	2.4	18.0	25.7	90.5	<0.1
C1u (21-35)	7.0	0.5	-	0.3	0.3	9.9	13.7	2.5	22.1	26.6	90.7	<0.1
Cgu2 (35-52)	6.6	0.4	-	0.3	0.3	8.9	19.5	3.0	23.4	32.0	90.8	1
2Chu3 (52-60+)	7.3	4.6	-	0.5	0.1	15.0	15.2	2.2	45.9	32.9	93.4	<0.1
P20: Hyperskeletic Spolic Technosol (Hyperhumic, Loamic, Somerimollic)												
Auh1 (0-5)	7.2	12.2	0.55	0.2	0.5	16.9	16.4	2.2	42.4	36.1	93.9	<0.1
Auh2 (5-11)	7.2	8.0	0.65	0.2	0.3	15.7	13.6	2.2	31.1	32.0	93.0	<0.1
AChu1(11-29)	7.3	7.7	1.1	0.3	0.2	17.3	13.3	2.7	54.3	33.9	91.9	<0.1
AChu2 (29-60+)	7.1	7.4	1.2	0.3	0.1	21.4	11.6	2.5	56.7	36.0	93.1	<0.1

Table 3. Grain size distribution of SC2, SC6 and P20 profiles

Horizon/depth	Coarse artefacts	Medium artefacts	Fine artefacts	Fine earth	Sand	Silt	Clay
	---------------------------------% ($v\ v^{-1}$)			------------------------	---------------	$g\ kg^{-1}$	------------
SC2: Hyperskeletic Spolic Technosol (Clayic)							
Au (0-7)	18	32	35	15	122	387	492
Cu1 (7-20)	29	41	20	10	131	398	471
Cu2 (20-33)	19	56	17	9	126	391	483
Cu3 (33-52)	11	44	31	13	85	405	510
Cu4 (52-70+)	19	69	8	4	87	421	503
SC6: Hyperskeletic Spolic Technosol (Clayic, Endoraptic)							
Au (0-9)	8	38	36	18	131	359	509
CAu (11-21)	16	54	23	8	183	343	474
C1u (21-35)	38	43	14	4	219	349	432
C2u (35-52)	27	53	13	7	74	406	521
2Cu (52-60)	0	55	35	9	358	383	260
P20: Hyperskeletic Spolic Technosol (Hyperhumic, Loamic, Somerimollic)							
A1u (0-5)	23	22	22	33	390	395	215
A2u (5-11)	19	31	27	23	434	358	209
AC1u (11-29)	25	29	28	18	490	308	202
AC2u (29-60+)	18	48	19	15	550	249	201

2.3.2. Micromorphology and SEM-EDS

Micromorphological data evidences significant differences between the microstructures of the studied Technosols (Table 4). SC2 0-10cm sample present four small zones (approximately 10% of the thin section area) where pedoplasmation is occurring, leading to a saprolite-like microstructure formed by pseudo-aggregates, resulting in a blocky angular microstructure (Fig. 3a and b). The grade of pedality is moderately developed and the faces of internal aggregates are accommodated to each other. Fragments of the original siltstone structure appear in the groundmass indicating an early stage of weathering. Groundmass and siltstones fragments color are similar (yellowish brown, 10YR 5/6) and the b-fabric is undifferentiated or striated. Few typic and irregular iron nodules appear (mean ø= 0.75mm) and Fe hypocoatings are absent (Fig. 3a and b).

ACu horizon in SC6 shows more abundantpedoplasmation zones, occurring in seven independent zones (approximately 30% of the thin section area). The grade of pedality in these zones is moderately to strongly developed, composing a subangular blocky primary structure (Fig. 3c and d). Groundmass color differs from SC2, presenting areas varying from reddish yellow to red, with stipple speckled b-fabric and Fe hypocoatings (Fig. 7c, d and Fig. 8b, c). Channels and vughs appear more often, associated with biological activity by roots (Fig 3d). Iron nodules are few and varying in type. Few typic (ø= 0.75mm) and irregular (ø= 1.1mm) and very few disjointed (ø= 0.7mm) nodules are seen (Fig. 4 and 8).

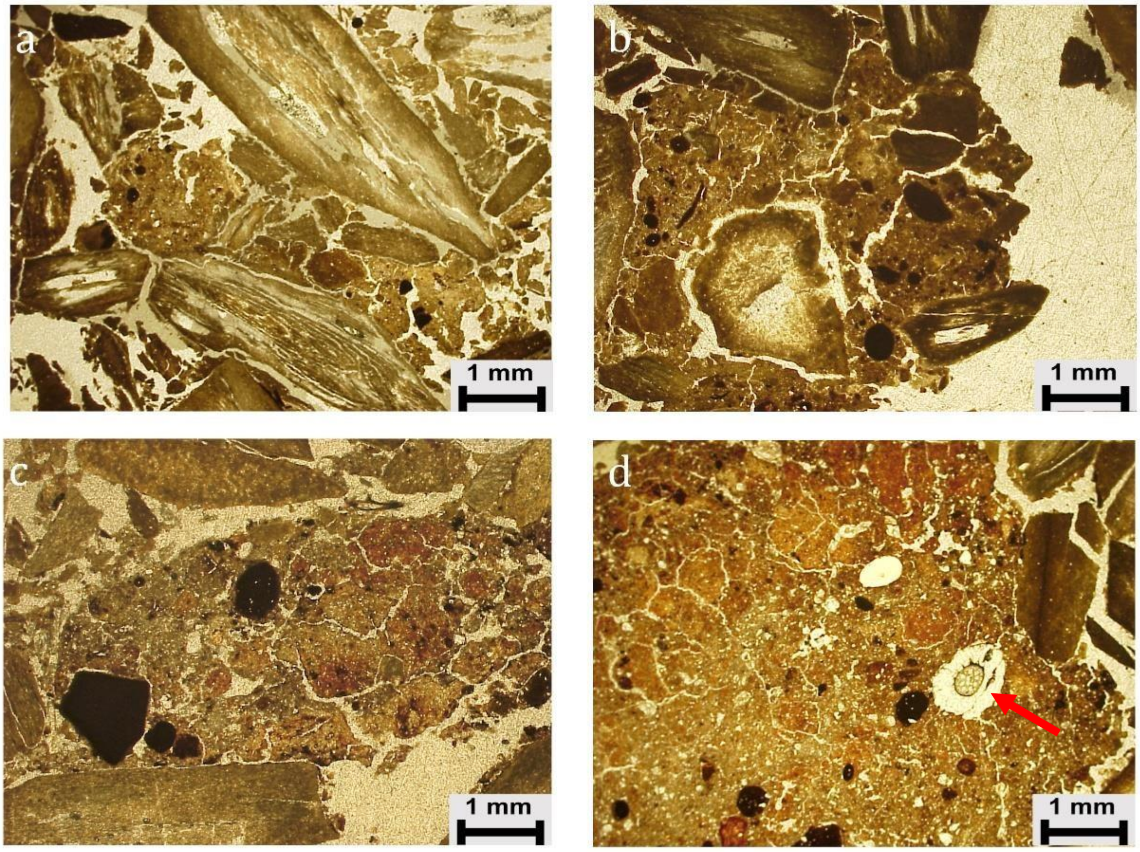

Fig. 3) Pseudo-aggregates in SC2 and SC6. Images (a) and (b) represent the SC2 angular blocky microstructure of pseudo-aggregates in initial stage of pedoplasmation. Siltstones remnants are still visible at the groundmass and matrix color resembles that of the rock. Images (c) and (d) are the subangular blocky microstructures in a in SC6. At the external walls of peds and intra-aggregates Fe is oxidizing as hypocoatings. Little of the siltstone structure is visible in the reddish yellow groundmass, indicating a more advanced degree of pedoplasmation facilitated by root activity (red arrow in d).

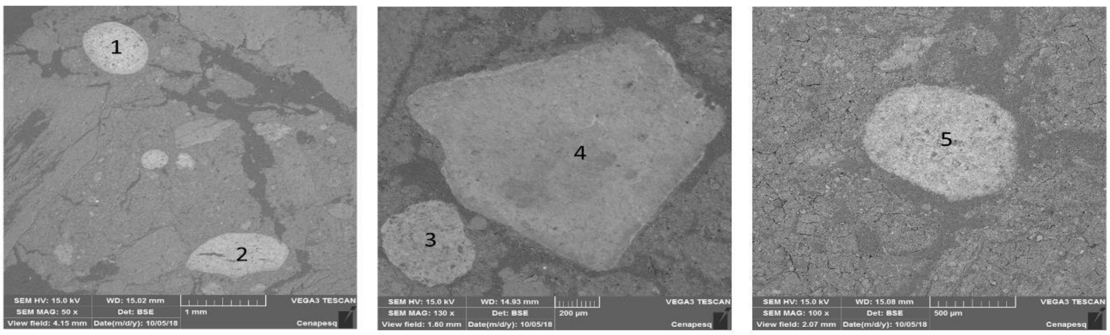

	% atomic	O	Si	Al	Fe	K
SC3	nodule 1	45,20	15,68	3,39	35,45	0,28
	nodule 2	51,23	6,27	6,40	35,69	0,41
SC7	nodule 3	34,31	22,51	1,46	41,23	0,50
	nodule 4	22,46	6,01	3,29	68,24	-
P20	Nodule 5	43,08	16,34	4,11	36,21	0,26

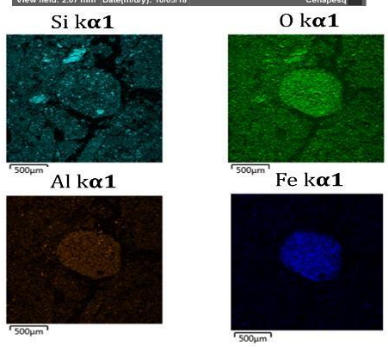

Fig4.) Composition of some nodules from SC2, SC6 and P20.

Redoximorphic features were evidencied in the Cgu2 horizon of SC6 (Fig. 4a and b). Iron oxides coatings and hypocoatings appear along voids and Fe and clay depletions inside aggregates. Some of the nodules seem to be degrading, as the boundary to the groundmass is more diffuse and they are less opaque. At the boundary of Cgu2 to 2Chu3 rhombohedral pyrite crystals were found inside silex, in association to black shale fragments.

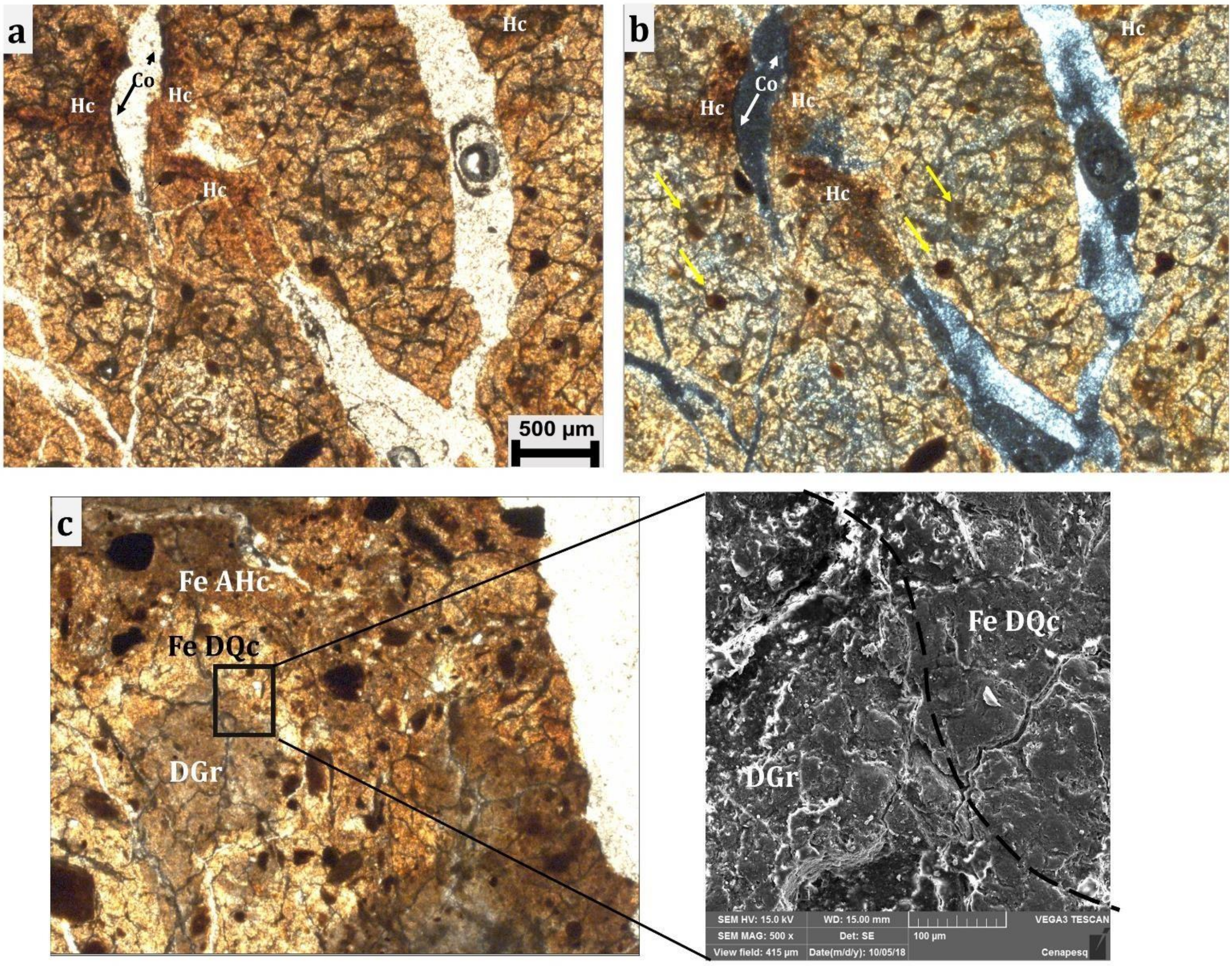

% atomic	O	Si	Al	Fe	K	Mg	Ca	Ti
Fe DQc	43,1	31,4	14,1	5,7	3,1	1,7	0,5	0,6
D Gr	55,1	27,8	9,6	3,9	2,2	1,1	0,3	0,3

Fig. 5) Redoximorphic features in SC6 Cgu2 horizon. (a) Fe coatings (C) and hypocoatings (Hc) along a channel void (ppl); (b) Diffuse boundary on degrading nodules (yellow arrows) and Fe precipitation as infillings along intrapedal voids (xpl); (c) Interior of a ped with depleted groundmass (DGr), Fe depletion quasicoating (Fe DQc) and Fe accumulation hypocoating towards a void. The internal nodules are degrading and have a diffuse boundary to the groundmass. The table shows the elemental composition of the pedofeatures. Note the lower concentration of Al and Fe in DGr, indicating both Fe and clay depletion.

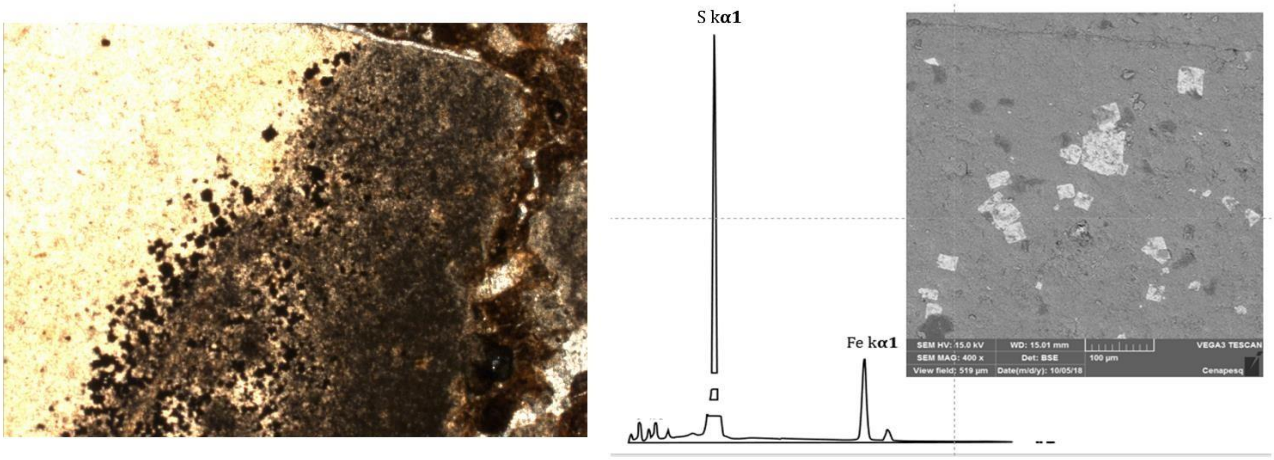

Fig. 5) Rhombohedral pyrite crystals inside a silex fragment, associated to black shales, at the boundary of Cgu2 to 2Chu3 horizons in SC6 profile.

P20 thin section showed a blocky subangular structure evolving to a crumb structure (Fig. 6a), with aggregates separated in an enaulic c/f-related distribution. Roots appear both intra and inter aggregates. The thin section presents complex porosity composed by channels, vughs and packing voids. The groundmass is dark brown (10YR 2.5/2), pigmented by organic matter with undifferentiated b-fabric. Excrement pedo- features can be seen in Fig 6c as loose continuous infilling of a void containing moderately coalesced ellipsoids excrements. Black shale fragments predominate followed by siltstones, some dolomitic limestone and rare apatite fragments (Fig 6d). The degree of weathering in black shales is higher than in siltstones. The latter are subangular fragments moderately weathered coated with finer material, presenting unfilled cracks, whereas black shales presented generalized cracks followed by a parallel linear fragmentation where pedoplasmation seems to be facilitated. Pyrite crystals were also found in this profile overlying silex fragments, suggesting that pyrite is associated to the black shales

.

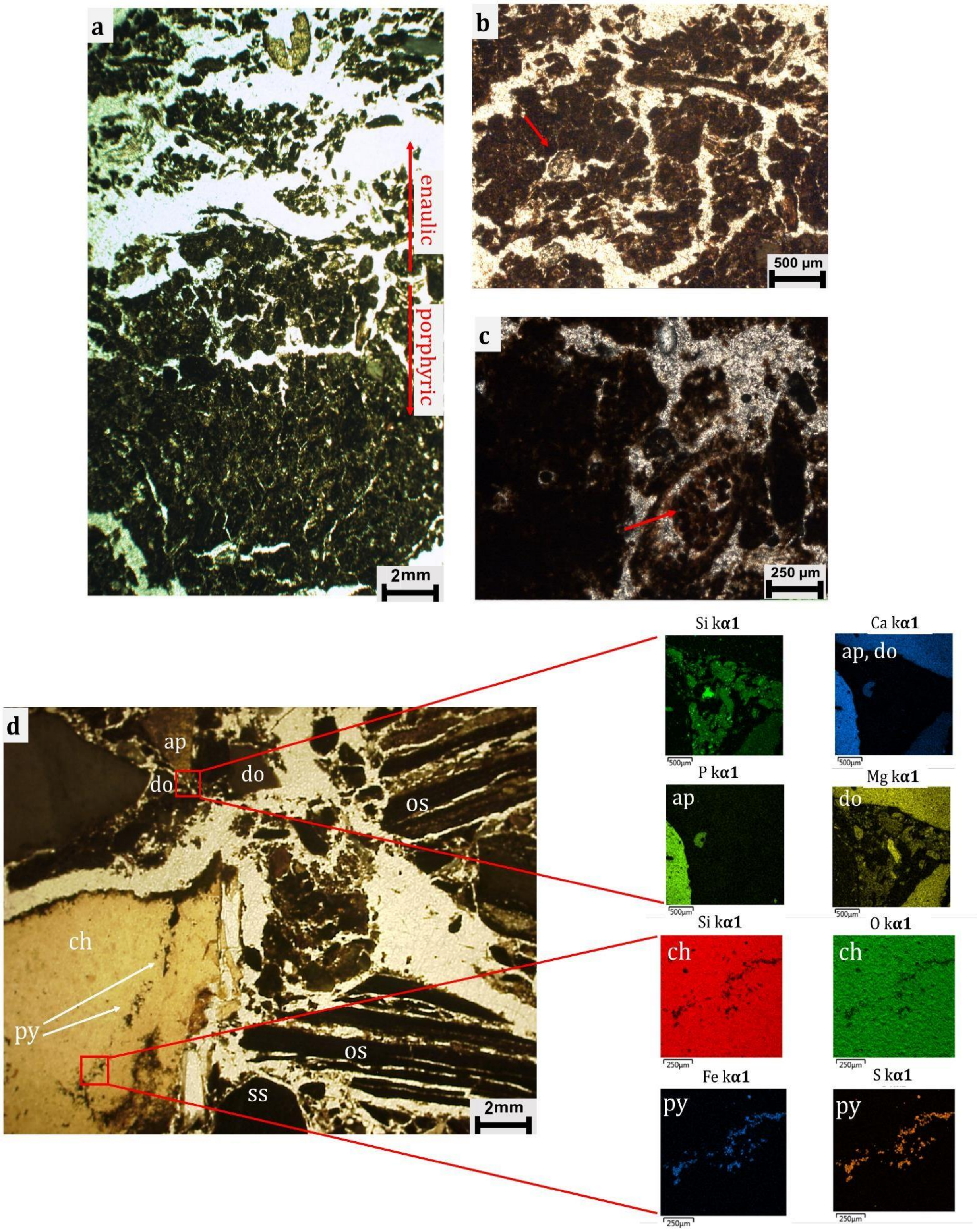

Fig. 6) P20 microstructure and features: (a) subangular blocky structure with open porphyric c/f related distribution evolving to an enaulic crumb structure in Au; (b) Living and decomposing roots favoring aggregation through bioturbation and organic matter addition; (c) Void filled with excrements as a record of faunal bioturbation; (d) artefacts diversity in P20: silex (ch) with pyrite crystals (py), dolomite (do), apatite (ap), black shale (os) and Siltstones (ss).

Table 4. Micromorphological description of SC2 (0-10cm), SC6 (0-10cm) and (50-60cm) and P20 (0-10cm)

Features	SC2 (0-10cm)	SC6 (0-10cm)	SC6 (50-60cm)	P20 (0-10cm)
Groundmass	90% Monic; 10% open porphyric with undiffered b-fabric	70% Monic; 30% open porphyric withstipple speckled b-fabric	80% Monic and 20% open porphyric withundiffered b-fabric	50% Monic. 30% Open porphyric; 20% enaulic; undiffered b-fabric
Microstructure	Single grain/ Angular blocky structure	Single grain/ Subangular blocky structure	Single grain/ Angular blocky structure	Single grain/ Subangular blocky and crumb structure
Basic mineral components	Coarse fraction: very coarse silstones fragments and quartz Fine fraction: anisotropic mineral, yellowishbrown (10YR 5/6)	Coarse fraction: very coarse siltstones fragments and quartz Fine fraction: anisotropic mineral, reddish yellow (5 YR 6/8), red (2.5 YR 4/6)	Coarse fraction: very coarse siltstones fragments and quartz Fine fraction: anisotropic mineral, reddish yellow (5 YR 6/8), gray mottles (10YR 6/1)	Coarse fraction: very coarse black shales, siltstones and dolomite fragments and quartz Fine fraction: isotropic organo-mineral, dark brown (10YR 2.5/2)
Pedofeatures	Amorphous: Few typic and irregular iron nodules with sharp boundary	Amorphous: Few typic and irregular (sharp boundary) and very few disjointed iron nodules diffuse boundary); Fe hypo and quasi-coatings	Amorphous: Few typic and irregular iron nodules (diffuse boundary), Fe coatings and hypocoatings, Fe depletion hypocoatings	Amorphous: Very few typic and irregular iron nodules. Excrement: loose continuous infillings, elipsoidal, moderate coalescence

2.4. Discussion

2.4.1 Macromorphology and physico-chemical attributes

Since parent materials of technosols grown with sugar cane are very similar in upper horizons it is possible to establish a chronosequence to assess the morphological evolution from SC2 to SC6. A longer period of plant activity was responsible for thickening the ACu horizon in SC6 and the development of CAu. The moderated medium granular structure and weak fine subangular blocky structure that appears in the SC6 ACu horizon is a result of root activity. After sugar cane harvest, growth of new roots with maintenance of part of the old system elevates belowground mass in the soil promoting aggregation (Smith et al., 2005). TOC is slightly higher in SC6 probably due to dead roots microbially mediated decomposition and exudation of organicacids in the rhizosphere (Drever and Vance, 1994). Root growth on the outsides of a forming ped, in combination with microbial extracellular substances and root exudates of plants, promotes the coalescence of loose soil material and cohesiveness of the peds (Hole and Nielsen, 1970).

Red and reddish yellow mottles that appear mostly in SC6 are probably due to oxidation of pyrites and saprolite-like soil matrix. Roots penetrate through siltstones and black shale fragments cracks accelerating oxidation and weathering (see Fig. 4a and b in annexes). Longer exposure to surface conditions and aeration led oxidation of Fe compounds of rock fragments to secondary Fe oxides.

Changes of chemical attributes in 2Chu3 of SC6 is due the nature of mine spoils. This horizon is composed essentially from black shale fragments which contain organic matter responsible from TOC increase (Santos, 2018). In addition, the presence of carbonates and phosphates associated to the black shale explains the higher pH and P values (Fig. 6d). Except for TOC content, physico-chemical attributes of 2Chu3 (SC6) are similar to those of the P20 profile.

In P20, the increase of fine earth towards the surface may be a consequence of longer biochemical weathering and organic matter decomposition (Fig. 6c). The development of a dark and well developed Au horizon in P20 is due to the addition of humified organic matter by melanization process (Anderson, 1987). High TOC content is explained in part by the addition of organic matter *in situ* from decomposition of roots and dead organism, a typical process of grasslands (Fenton, 1983). Black shale organic matter may also contribute to elevate TOC values, since organic carbon content of these rocks average 3.8% in the Assistencia Member of Irati Formation (Santos, 2018). In fact, 2Chu3 horizon in SC6, which is composed mainly by black shales, presented 4.2% of TOC (Table 2). Despite the lowest clay content, CEC values in P20 were higher than in SC2 and SC6 due to organic matter addition.

The intense root activity was expected to reduce the pH values in soil solution as observed in SC6, instead, it remained close to neutral. Particularly in P20, small fragments of dolomitic rock rich in $CaMg(CO_3)_2$ were found (Fig. 6d), probably associated to the black shale (Lages, 2004). When exposed to the action of microorganisms and root exudates carbonate minerals tend to have their dissolution increased, which buffers acidification (Uroz et al. 2009).

2.4.2. Pedoplasmation

At the micromorphological scale, differences in aggregation and weathering are evident when comparing SC2 and SC6 thin sections. The main process occurring in these soils is pedoplasmation, which consists of the *in situ* development of a structured, loose material where the original fabric of the saprolite is no longer visible (Stoops and Schaefer, 2010). Some basic concepts must be enlightened since pedoplasmation concept concerns to saprolite or sediment transformations. Because saprolite by definition is the *in situ* weathered bedrock (Stolt and Baker, 1995), it cannot be transported. In our case, though, the rock fragments, i.e. mine spoils, were artificially broken and transported from their original location. These fragments have a larger specific surface area and are more exposed to the surface than saprolite, which may increase their weathering rate. Nevertheless, the nature of processes that take place in these mine spoils is very similar to those occurring in saprolites, allowing the pedoplasmation approach to support pedogenesis in the studied technosols.

When pedoturbation is still little pronounced and aggregates conserve much of the rock fragment's morphology, we will refer them as pseudo-aggregates or pseudo-peds. Differently from true pedogenetic peds, the intrapedal planar voids in pseudo-aggregates and accommodated intra-aggregates indicate they were formed mainly due mechanical stress rather than chemical weathering (Zauyah et al., 2018). A higher degree of pedoplasmation was observed in SC6 pseudo-aggregates compared to SC2, evidenced by redder matrix color and moderate to strong grade of pedality (Fig. 7). Higher biological activity, e.g. growth of roots, and the preferential paths for weathering solutions, due to development of the initial planal voids, led to more rounded faces in SC6 pseudo-aggregates, giving rise to subangular blocky peds. Also, it can be observed in Fig. 7 that the original striated b-fabric of the siltstones is disappearing in SC6 giving place to stipple speckled b-fabric, indicating clay randomization and neoformation of secondary clay minerals (Kühn et al., 2018; Stoops et al., 2010). On the other hand, SC2 pseudo-aggregates are weakly developed and still contain many siltstone fragments, conserving much of the saprolite b-strial fabric.

While the groundmass color of SC2 pseudo-aggregates is brownish yellow indicating a silt-rich fine material (Bullock et al., 1985), in SC6 iron mobilization pedofeatures appear in a more reddish yellow matrix color with the occurrence of Fe hypo and quasicoatings (Fig. 7c and d). The juxtaposition of less pigmented and dark red or opaque zones rich in iron oxides is common in saprolites, which after pedoplasmation form a uniform reddish or reddish yellow material (Muggler & Buurman, 1997). These micromorphological observations evidence that chemical weathering and mineral transformations are more advanced in SC6 than SC2.

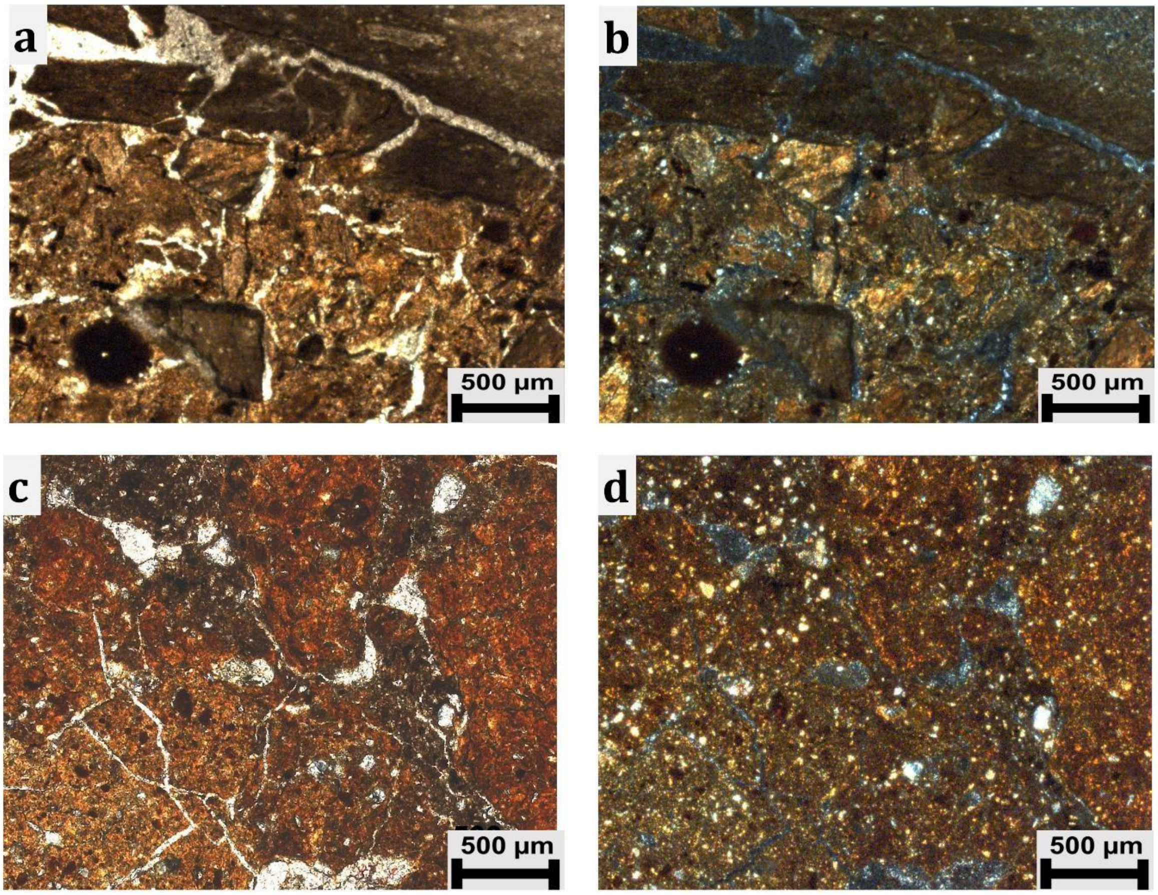

Fig.7) Groundmass comparison between SC2 and SC6. (a) brownish yellow groundmass with siltstones fragments remnants in SC2 (ppl); (b) Striated b-fabric in SC2 resembling that of the original siltstone b-fabric (xpl); (c) red and reddish yellow groundmass in SC6 with strong pedality (ppl); (d) stipple speckled b-fabric as a result of advanced pedoplasmation in SC6.

In P20, black shale fragments present higher degree of alteration than siltstones suggesting that pedoplasmation is more intense in the former. The greater amount of black shales and biological activity (Fig. 6c) in this profile contributes to a more developed structure. The original rock structure is little evident in peds, noticed by the disappearance of the parallel arrangement typical of shales, which is mainly a consequence of pedoturbation (Stoops and Schaefer, 2010). Bioturbation features promoted both by plants and soil fauna can be checked in Fig 6c. This process is very important to the transformation of the saprolite-like fabric, homogenization of the groundmass and generation of voids. The intense biological activity is responsible for the evolution from subangular blocky to crumb structure with an organo- mineral fabric.

2.4.3. Ferruginous pedofeatures

Since iron nodules are found inside siltstones fragments, they can be considered relict pedofeatures. Additionally, the sharp boundary separating the preserved nodules and the groundmass suggest they are not contemporary, classifying them as anorthic iron nodules (Tucker et al., 1993). The digitated and disjointed shapes of weathered Fe nodules and the depletion hypocoatings along their sides denote they are not forming, but actually degrading (Lindbo et al., 2010).

Iron nodule dissolution seems to contribute significantly to the groundmass ferruginous pigmentation, i.e. rubification, especially in SC6 surface horizon. The hypo-coatings that appear in aggregate walls in ACu horizon are probably due to the reprecipitated iron oxides derived from Fe nodules dissolution. This cannot be interpreted as a redox originated process because the lack of Fe depletion features appoints there is no seasonal water saturation (Lindbo et al., 2010). However, Fe nodules degradation may be plant induced. In fact, low molecular weight organic acids exuded by plant roots are reported to form soluble complexes with iron, enhancing weathering (Jones et al., 1996; Lundström et al., 2000). Pedoturbation may also contribute to nodules destruction via fragmentation to smaller pieces (Fig. 8b).

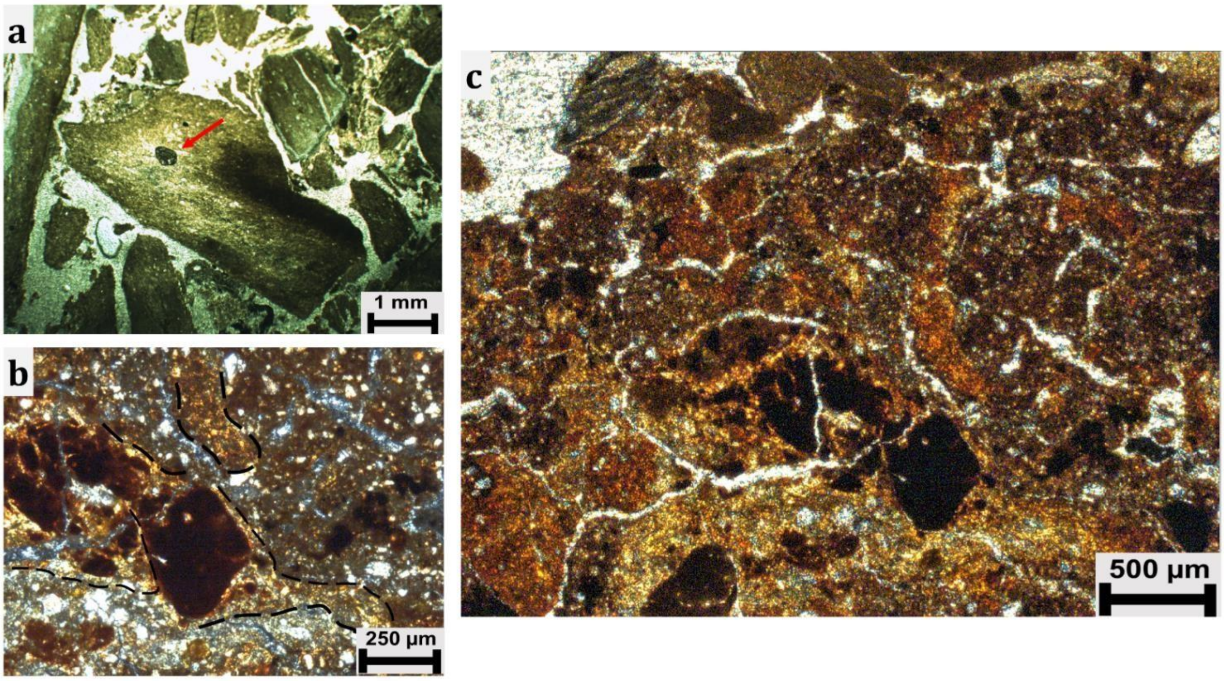

Fig. 8) Nodules and Fe mobilization; (a) Nodule inside a siltstone fragment as evidence of an inherited pedofeature; (b) Nodule dissolution and fragmentation in SC6 and Fe mobilization towards the groundmass as quasicoatings impregnations; (c) Pigmentation of the groundmass (Fe quasicoatings and hypocoatings) due to nodules dissolution.

At the bottom of SC6 redoximorphic conditions are clearly present. The presence of a low-permeability layer composed of very large black shale fragments immediately below the 2Cu horizon hampers water drainage. The well-marked wet and dry seasons mayalso favor periods of water saturation in the SC6 profile. During the wet season the lower part of the profile remains saturated for longer periods of time and redoximorphic features can be produced in aggregates of the Cgu2 horizon (Fig. 4a, b and c). In this case, nodules degradation is caused by redox process. In fact, Fe nodules dissolution is more advanced in the interior of peds where oxygen diffusion is restricted and anoxic conditions remain. Alternating wet and dry periods favors Fe redox cycles, causing Fe to precipitate in intra-aggregates infillings. The oxidation of the rhombohedral pyrite crystals found at the Cgu2-2Chu3 boundary may also contribute to matrix pigmentation. The exposure of pyrite to oxidizing conditions releases H^+ and ferric sulfates, which may be partially or totally hydrolyzed to produce Fe oxides (Fanning et al., 2002). Pyrite oxidation also helps to explain lower pH values in Cgu2.

2.4.4. Melanization

Melanization is the main pedogenic process occurring in P20. Key factors for formation of the mollic epipedon are: the proliferation and decay of grass roots as an important input of organic matter; and faunal activity (Fig. 6c) contributing to the rapid organicmatter incorporation and thickening of the mollic horizon through bioturbation.

Mollic epipedons are typical of temperate grasslands of mid-latitudes and are formed by long-term melanization process. However, the intensity of melanization process are not common in the present climatic settings. Additionally, soil organic carbon content in P20 is not usual for mollic epipedons.

We hypothesize the follow: i) there is a rapid decomposition of raw organic matter to humus; ii) microbial byproducts are an important source of diverse organic carbon; iii) stabilization is mediated by Ca- organic matter complexes; iv) the presence of gravels favors organic matter incorporation in depth.

An accelerated microbial decomposition is transforming raw organic matter quickly to humus, which remains stabilized due to the formation of organo-mineral complexes. The intense root exudation is an input of easily decomposable organic matter that stimulates a fast response of microbial activity as a rhizosphere priming effect (Merino et al., 2015). Consequently, high energy and high nutrient availability increase organic matter decomposition rate (Bingeman et al., 1953).

The heterogeneity of organic matter chemical composition influences its stabilization potential and interaction with clay minerals, thus, favoring accumulation (Kallenbach et al., 2016; Malik et al., 2016). It has been demonstrated that even in the absence of chemically diverse plant inputs, i.e. low plant diversity, organic matter chemical heterogeneity can originate from microbial metabolism byproducts (Throckmorton et al., 2012).

Organic matter stabilization is also probably favored in P20 because of high amounts of Ca^{2+}. Many studies have highlighted the strong correlation between exchangeable Ca^{2+} and TOC content (Bertrand et al., 2007; Clough and Skjemstad, 2000; Muneer and Oades, 1989; Oades, 1993; Six et al., 2004). Calcium also stimulates the decomposition of fresh organic materials, but may slow the decomposition of humus and highly humified substances (Rowley, 2018). The high amount of Ca^{2+} in P20 is responsible for stabilizing organic matter probably due to occlusion and organo-cation interactions. The first is a consequence of the positive effect on soil aggregation promoted by exchangeable calcium (Bakker and Emerson, 1973; Bronick and Lal, 2005; Muneer and Oades, 1989), as a significant proportion of biologically active organic carbon in soil remains physically protected from decomposition inside the aggregates (Lützowet al., 2006). The latter refers to ligand exchange and chelation mechanisms between Ca^{2+} organic functional groups (Mortensen, 1963) forming inner sphere complexes which chemically stabilizes organic matter (Rowley, 2018).

The incorporation of organic matter with depth may also be explained by the strong correlation between TOC and coarse fragment content (Schaetzl, 1991). As the surface area decreases, melanization can operate more deeply into the gravelly soil as Ca-organic coatings on coarse particles (Protz, 1983). Additionally, deeper rooting facilitated through roots growth in inter-gravel voids favors melanization and thus A horizon thickening. Furthermore, the fine grained organo-mineral material which composes the black shales contributes to elevated TOC values and low chroma values as well.

2.5. Conclusions

Four years of pedogenesis were enough to trigger substantial differences in color and structure development. Pedoplasmation appear as the main process occurring in the first stage of pedogenesis and was clearly favored by the fragmentation of mine spoils and roots metabolism. Moreover, the artificial assemblage of the constructed soils affected drainage, leading to hydromorphic processes. A strong melanization process was evidenced after 20 years of pedogenesis accompanied by high organic carbon accumulation.

Morphological investigations, at a macro and microscopic levels, evidence a fast pedogenetic evolution in constructed technosols under the tropical pedo- environment. It is clear how human activity (soil construction and plant selection) may affect soil formation, triggering pedogenetic processes unusual for the local climatic condition. Thus, these study shows that soils suitable for land reclamation can be constructed by simply reusing limestone mine spoils to fulfill exploited mine pits.

References

Anderson D.W. 1987. Pedogenesis in the Grassland and Adjacent Forests of the Great Plains. In: Stewart B.A. (eds) Advances in Soil Science. Advances in Soil Science, vol 7. Springer, New York, NY

Asensio, V., Vega, F.A., Anadrade, M.L., Covelo, E.F., 2013. Technosols Made of Wastes to Improve Physico-Chemical Characteristics of a Copper Mine Soil. Pedosphere 23, 1–9. https://doi.org/https://doi.org/10.1016/S1002-0160(12)60074-5

Bakker, A.C., Emerson, W.W., 1973. The comparative effects of exchangeable calcium, magnesium, and sodium on some physical properties of red-brown earth subsoils. III. The permeability of Shepparton soil and comparison of methods. Soil Res. 11, 159–165.

Bertrand, I., Delfosse, O., Mary, B., 2007. Carbon and nitrogen mineralization in acidic, limed and calcareous agricultural soils: Apparent and actual effects, Soil Biology & Biochemistry - SOIL BIOL BIOCHEM. https://doi.org/10.1016/j.soilbio.2006.07.016

Bingeman, C.W., Varner, J.E., Martin, W.P., 1953. The Effect of the Addition of Organic Materials on the Decomposition of an Organic Soil1. Soil Sci. Soc. Am. J. 17, 34–38. https://doi.org/10.2136/sssaj1953.03615995001700010008x

Brinkman, R., 1970. Ferrolysis, a hydromorphic soil forming process. Geoderma 3, 199–206. https://doi.org/https://doi.org/10.1016/0016-7061(70)90019-4

Bronick, C.J., Lal, R., 2005. Soil structure and management: a review. Geoderma 124, 3–22. https://doi.org/https://doi.org/10.1016/j.geoderma.2004.03.005

Bullock, P., Fedoroff, N., Jongerius, A., Stoops, G., Tursina, T., 1985. Handbook for soil thin section description. Waine Research, Wolverhampton.

Cambardella. C.A.. Gajda. A.M.. Doran. J.W.. Wienhold. B.J.. Kettler. T.A.. 2001. Estimation of particulate and total organicmatter by weight loss-on-ignition. In: Lal. R.. Kimble. M.. Follett. R.F.. Stewart. B.A. (Eds.). Assessment Methods for Soil Carbon. Lewis. BocaRaton. pp.349–359.

Capra, G.F., Ganga, A., Grilli, E., Vacca, S., Buondonno, A., 2015. A review on anthropogenic soils from a worldwide perspective. https://doi.org/10.1007/s11368-015-1110-x

CEPAGRI - Centro de Pesquisas Meteorológicas e Climáticas Aplicadas à Agricultura. Climas dos municípios paulistas. Available on: http://www.cpa.unicamp.br/outras-informacoes/clima_muni_509.html>.

Chesworth, W. (Ed.), 2008. Melanization BT - Encyclopedia of Soil Science. Springer Netherlands, Dordrecht, p. 449. https://doi.org/10.1007/978 -1-4020-3995-9_349

Clough, A., Skjemstad, J.O., 2000. Physical and chemical protection of soil organic carbon in three agricultural soils with different contents of calcium carbonate. Soil Res. 38, 1005–1016.

Drever, J.I., Vance, G.F., 1994. Role of Soil Organic Acids in Mineral Weathering Processes BT - Organic Acids in Geological Processes, in: Pittman, E.D., Lewan, M.D. (Eds.). Springer Berlin Heidelberg, Berlin, Heidelberg, pp. 138 –161. https://doi.org/10.1007/978-3-642-78356-2_6

Duchaufour, P., 1982. Weathering and clay formation BT - Pedology: Pedogenesis and classification, in: Duchaufour, P. (Ed.). Springer Netherlands, Dordrecht, pp. 5–27. https://doi.org/10.1007/978-94-011-6003-2_2

Fanning, M., Rabenhorst, M., Burch, S., Islam, K., Tangren, S., 2002. Sulfides and sulfates. Dixon Schulze (eds). Soil Mineral. with enviromental Appl. SSSA B. Ser. 7, 229–261. https://doi.org/10.12957/jse.2018.33304

Gee, G.W., Or, D., 2002. Particle-size analysis. in Mehtods of Soil Analysis, Part 4: Physical Mehtods.

Hinsinger, P., Plassard, C., Tang, C., Jaillard, B., 2003. Origins of root-mediated pH changes in the rhizosphere and their responses to environmental constraints: A review, Plant and Soil. https://doi.org/10.1023/A:1022371130939

Howard, J., 2017. Human Impacts on Soils BT - Anthropogenic Soils, in: Howard, J. (Ed.). Springer International Publishing, Cham, pp. 53–62. https://doi.org/10.1007/978-3-319-54331-4_4

Huot, H., Faure, P., Biache, C., Lorgeoux, C., Simonnot, M.-O., Morel, J.L., 2014. A Technosol as archives of organic matter related to past industrial activities. Sci. Total Environ. 487, 389–398. https://doi.org/https://doi.org/10.1016/j.scitotenv.2014.04.047

IBGE, 2012. Brazilian Institute of Geography and Statistics. Technical Handbook of the Brazilian Vegetation, (second ed.), Rio de Janeiro, ISSN 0103-9598

IUSS Working Group WRB, 2014. World reference base for soil resources 2014. International soil classification system for naming soils and creating legends for soil maps, World Soil Resources Reports No. 106. https://doi.org/10.1017/S0014479706394902

Jahn, R., Blume, H.P., Asio, V., Spaargaren, O., Schad, P., 2006. Guidelines for soil description, 4th edition.

Jangorzo, N.S., Watteau, F., Schwartz, C., 2013. Evolution of the pore structure of constructed Technosols during early pedogenesis quantified by image analysis. Geoderma 207–208. https://doi.org/10.1016/j.geoderma.2013.05.016

Jones, D.L., Darah, P.R., Kochian, L. V, 1996. Critical evaluation of organic acid mediated iron dissolution in the rhizosphere and its potential role in root iron uptake. Plant Soil 180, 57–66. https://doi.org/10.1007/BF00015411

Kallenbach, C.M., Frey, S.D., Grandy, A.S., 2016. Direct evidence for microbial-derived soil organic matter formation and its ecophysiological controls. Nat. Commun. 7, 13630.

Kühn, P., Aguilar, J., Miedema, R., Bronnikova, M., 2018. Chapter 14 - Textural Pedofeatures and Related Horizons, in: Stoops, G., Marcelino, V., Mees, F.B.T.-I. of M.F. of S. and R. (Second E. (Eds.), Elsevier, pp. 377–423. https://doi.org/https://doi.org/10.1016/B978-0-444-63522-8.00014-0

Lindbo, D. L., H. Stolt, M., J. Vepraskas, M., 2010. Redoximorphic Features, Interpretation of Micromorphological Features of Soils and Regoliths. https://doi.org/10.1016/B978-0-444-53156-8.00008-8

Lages, L.C., 2004. A Formação Irati (Grupo Passa Dois, Permiano, Bacia do Parana) no furo de sondagem FP-01-PR (Sapopema, PR) 117.

Lundström, U.S., van Breemen, N., Bain, D., 2000. The podzolization process. A review. Geoderma 94, 91–107. https://doi.org/https://doi.org/10.1016/S0016-7061(99)00036-1

Lützow, M. v., Kögel-Knabner, I., Ekschmitt, K., Matzner, E., Guggenberger, G., Marschner, B., Flessa, H., 2006. Stabilization of organic matter in temperate soils: mechanisms and their relevance under different soil conditions – a review. Eur. J. Soil Sci. 57, 426–445. https://doi.org/10.1111/j.1365- 2389.2006.00809.x

Malik, A.A., Roth, V.-N., Hébert, M., Tremblay, L., Dittmar, T., Gleixner, G., 2016. Linking molecular size, composition and carbon turnover of extractable soil microbial compounds. Soil Biol. Biochem. 100, 66–73. https://doi.org/https://doi.org/10.1016/j.soilbio.2016.05.019

Merino, C., Nannipieri, P., Matus, F., 2015. Soil carbon controlled by plant, microorganism and mineralogy interactions . J. soil Sci. plant Nutr. .

Morel, J.L., Chenu, C., Lorenz, K., 2014. Ecosystem services provided by soils of urban , industrial , traffic , mining , and military areas (SUITMAs). https://doi.org/10.1007/s11368-014-0926-0

Mortensen, J.L., 1963. Complexing of Metals by Soil Organic Matter1. Soil Sci. Soc. Am.J.27,179–186. https://doi.org/10.2136/sssaj1963.03615995002700020027x

Muneer, M., Oades, J.M., 1989. The role of Ca-organic interactions in soil aggregate stability .III. Mechanisms and models. Soil Res. 27, 411–423.

Murphy, C.P., 1987. Thin Section Preparation of Soils and Sediments, XF2006266776. https://doi.org/10.1097/00010694-198710000-00013

Oades, J.M., 1993. The role of biology in the formation, stabilization and degradation of soil structure, Geoderma. https://doi.org/10.1016/0016 -7061(93)90123-3

Pawlik, Ł., Šamonil, P., 2018. Biomechanical and biochemical effects recorded in the tree root zone – soil memory, historical contingency and soil evolution under trees. Plant Soil 426, 109–134. https://doi.org/10.1007/s11104-018-3622-9

Protz, R., 1983. Calcium-dominated organans in humic podzols from the hudson and James Bay Lowlands of Ontario (Canada). Geoderma 30, 171–177.

https://doi.org/https://doi.org/10.1016/0016-7061(83)90064-2

Robles-Arenas, V.M., Rodríguez, R., García, C., Manteca, J.I., Candela, L., 2006. Sulphide-mining impacts in the physical environment: Sierra de Cartagena–La Unión (SE Spain) case study. Environ. Geol. 51, 47–64. https://doi.org/10.1007/s00254-006-0303-4

Rodríguez-Vila, A., Asensio, V., Forján, R., Covelo, E.F., 2016. Assessing the influence of technosol and biochar amendments combined with Brassica juncea L. on the fractionation of Cu, Ni, Pb and Zn in a polluted mine soil. J. Soils Sediments 16. https://doi.org/10.1007/s11368-015-1222-3

Rodríguez-Vila, A., Covelo, E.F., Forján, R., Asensio, V., 2015. Recovering a copper mine soil using organic amendments and phytomanagement with Brassica juncea L.J. Environ. Manage. 147. https://doi.org/10.1016/j.jenvman.2014.09.011

Rodríguez-Vila, A., Forján, R., Guedes, R.S., Covelo, E.F., 2017. Nutrient phytoavailability in a mine soil amended with technosol and biochar and vegetated with Brassica juncea. J. Soils Sediments 17. https://doi.org/10.1007/s11368-016-1643-7

Rowley, M.C., 2018. Calcium-mediated stabilisation of soil organic carbon 27–49. https://doi.org/10.1007/s10533-017-0410-1

Santos, W., Bergasmachi, S., Santos, A.C., Rogrigues, R., Bertolino, L.C., 2018. Characterization of the Assistência Member, Irati Formation, Paraná Basin, Brazil: Organic matter and Mineralogy , 3, 36–45.

Schaetzl, R.J., 1991 Factors affecting the formation of dark, thick epipedons beneath forest vegetation, Michigan, USA. J. Soil Sci. 42, 501–512. https://doi.org/10.1111/j.1365-2389.1991.tb00426.x

Scholtus, N., Echevarria, G., Florentin, L., Bonis, M.-L., De Donato, P., Simonnot, M.-O., Morel, J.-L., 2015. Expected evolution of a Technosol derived from excavated Callovo-Oxfordian clay material. J. Soils Sediments 15, 332–346. https://doi.org/10.1007/s11368-014-1020-3

Séré, G., Schwartz, C., Ouvrard, S., Renat, J.C., Watteau, F., Villemin, G., Morel, J.L., 2010. Early pedogenic evolution of constructed Technosols. J. Soils Sediments 10, 1246–1254. https://doi.org/10.1007/s11368-010-0206-6

Six, J., Bossuyt, H., Degryze, S., Denef, K., 2004. A history of research on the link between (micro)aggregates, soil biota, and soil organic matter dynamics. Soil Tillage Res. 79, 7–31. https://doi.org/https://doi.org/10.1016/j.still.2004.03.008

Smith, D.M., Inman-Bamber, N.G., Thorburn, P.J., 2005. Growth and function of the sugarcane root system. F. Crop. Res. 92, 169–183. https://doi.org/https://doi.org/10.1016/j.fcr.2005.01.017

Sokolov, D.A., Androkhanov, V.A., Kulizhskii, S.P., Domozhakova, E.A., Loiko, S. V, 2015. Morphogenetic diagnostics of soil formation on tailing dumps of coal quarries in Siberia. Eurasian Soil Sci. 48, 95–105. https://doi.org/10.1134/S1064229315010159

Stolt, M.H., Baker, J.C., 1995. Strategies for studying saprolite and saprolite genesis, International Journal of Rock Mechanics and Mining Sciences and Geomechanics Abstracts. https://doi.org/10.1016/0148-9062(95)90087-L

Stoops, G., de Melo Marcelino, V., Mees, F., 2010. Interpretation of Micromorphological Features of Soils and Regoliths. https://doi.org/10.1016/C2009-0-18081-9

Stoops, G., E.G.R. Schaefer, C., 2010. Pedoplasmation. https://doi.org/10.1016/B978-0-444-53156-8.00005-2

Swenson, J.J., Carter, C.E., Domec, J.-C., Delgado, C.I., 2011. Gold Mining in the Peruvian Amazon: Global Prices, Deforestation, and Mercury Imports. PLoS One 6, e18875.

Szabó, J., 2010. Anthropogenic Geomorphology: Subject and System BT - Anthropogenic Geomorphology: A Guide to Man-Made Landforms, in: Szabó, J., Dávid, L., Lóczy, D. (Eds.), . Springer Netherlands, Dordrecht, pp. 3–10. https://doi.org/10.1007/978-90-481-3058-0_1

Thornton, E.B., Sallenger, A., Sesto, J.C., Egley, L., McGee, T., Parsons, R., 2006. Sand mining impacts on long-term dune erosion in southern Monterey Bay. Mar. Geol. 229, 45–58. https://doi.org/https://doi.org/10.1016/j.margeo.2006.02.005

Throckmorton, H.M., Bird, J.A., Dane, L., Firestone, M.K., Horwath, W.R., 2012. The source of microbial C has little impact on soil organic matter stabilisation in forest ecosystems. Ecol. Lett. 15, 1257–1265. https://doi.org/10.1111/j.1461-0248.2012.01848.x

Tucker, R.J., Drees, L.R., Wilding, L.P., 1993. Signposts old and new; active and inactive redoximorphic features; and seasonal wetness in two Alfisols of the gulf coast region of Texas, U.S.A., in: Ringrose-Voase, A.J., Humphreys, G.S.B.T.-D. in S.S. (Eds.), Soil Micromorpohlogy: Studies in Management and Genesis. Elsevier, pp. 149–159. https://doi.org/https://doi.org/10.1016/S0166-2481(08)70405-7

Zauyah, S., Schaefer, C.E.G.R., Simas, F.N.B., 2018. Chapter 3 - Saprolites, in: Stoops, G., Marcelino, V., Mees, F.B.T.-I. of M.F. of S. and R. (Second E. (Eds.), . Elsevier, pp. 37–57. https://doi.org/https://doi.org/10.1016/B978-0-444-63522-8.00003-6

3. RHIZOSPHERE-INDUCED WEATHERING IN CONSTRUCTED TECHNOSOLS

Abstract

Besides sustaining important processes in developing of plants, the rhizosphere promotes chemical changes that deeply influence on the dynamics of mineral dissolution and neoformation. This effect can be very expressive in incipient soils, such as Technosols which contain significant amounts of weatherable minerals. In this study we characterized the rhizosphere and the bulk soil of three constructed Technosols developed from dolomitic mine spoils and planted with tropical grasses. The main artefacts in these soils were siltstones and black shales fragments. We evaluated the chemical, microbiological (soil enzymes) attributes and the mineralogy of silt and clay fractions of rhizosphere and bulk soil. We found that the higher dissolved organic matter contents and microbial activity were associated to rhizospheric soils and, thus, a higher degree of primary minerals weathering. Geochemical data and XRD patterns evidence the neoformation of secondary clays in the rhizosphere pedoenvironment, coupled to the microbiological activity.

Keywords: Technogenic soils; Mine spoils; Soil mineralogy; Microbiology; Soil enzymes

3.1. Introduction

Technosols are soils derived from anthropic activities and, thus, are prone to form in the mining enviroment (IUSS Working Group WRB, 2014). They are usually incipient soils and subjected to the same factors of soil formation as natural soils (Leguedois, 2016), but may weather more rapidly due to the peculiar chemical, mineralogical, and physical properties of their technogenic materials, i.e. artefacts (Huot, 2015).

Plants and their associated microorganisms (bacteria and fungi, mainly) are important weathering agents, which promote chemical changes in the soil solution, affect mineral dissolution and neoformation processes (Lucas, 2001). When considering the rhizosphere, the effect of plants on soils is even more intense. Primary minerals dissolution mediated by organic acids are up to 10 times higher than dissolution via inorganic acids solutions (Welch and Ullman, 1993).

Defined as the volume of soil affected by the activity of roots of the living plants, the rhizosphere provides a favorable environment for the growth of microorganisms (Hartmann et al., 2008). The exudation of specific organic compounds affects the structural and functional diversity of microbial community, promoting the intensification of microbial activity (Nannipieri et al., 2008). Consequently, the rhizosphere environment and its associated microbiota plays a major role in the developing of plants. Synthesis of phytohormones to suppress abiotic stresses, the production of siderophores to increase iron uptake, the biological nitrogen fixation and mineral dissolution to provide the inorganic nutrients for plant establishment and growth are some of the ways in which plants can benefit from rhizosphere microorganisms (Crowley, 2006; Egamberdieva et al., 2017; Gaskins et al., 1985; Jongmans et al., 1997). These rhizosphere-mediated processes are also of ecological importance (Mapelli et al., 2012).

Considering that the microbial community of the rhizosphere varies according to the plant species and soil type (Garbeva et al., 2008), it is important to evaluate the rhizosphere effect on pedogenesis of Technosols given the various possibilities of combining plants and artefacts. Assessing the rhizosphere environment separately from the bulk soil allows to evidence the most direct effect of plants and associated organisms in promoting Technosols weathering.

When it comes to incipient soil development, containing large amounts of primary minerals, the rhizosphere is expected to play a central role in weathering and mineral alterations in Technosols. Thus, the objectives of this study were (1) to compare the biogeochemical environment of the rhizosphere of tropical grasses with the bulk soil and (2) to investigate the rhizosphere effect on the mineralogical transformations of Technosols constructed with dolomitic limestone mine spoils.

3.2. Materials and methods

3.2.1. Study area

The study was conducted in three rehabilitated open casts areas at a limestone mine in SE São Paulo, Brazil (Fig. 1). For 20 years, *Brachiaria spp* has been grown in one of the sites (P20) and the two newest areas were plated with sugar cane, for 2 and 6 years (SC2 and SC6). The mine spoils are composed mainly by grayish siltstones, pyritic black shales, silex pebbles and dolomite fragments from the Irati Formation. According to Koeppen classification system, the regional climate is humid-subtropical (Cwa). The average annual temperature is 21.4ºC. Annual rainfall is 1.213 mm, mostly concentrated between November and March (CEPAGRI). The natural vegetation consists of semi-evergreen forest (IBGE 2012).

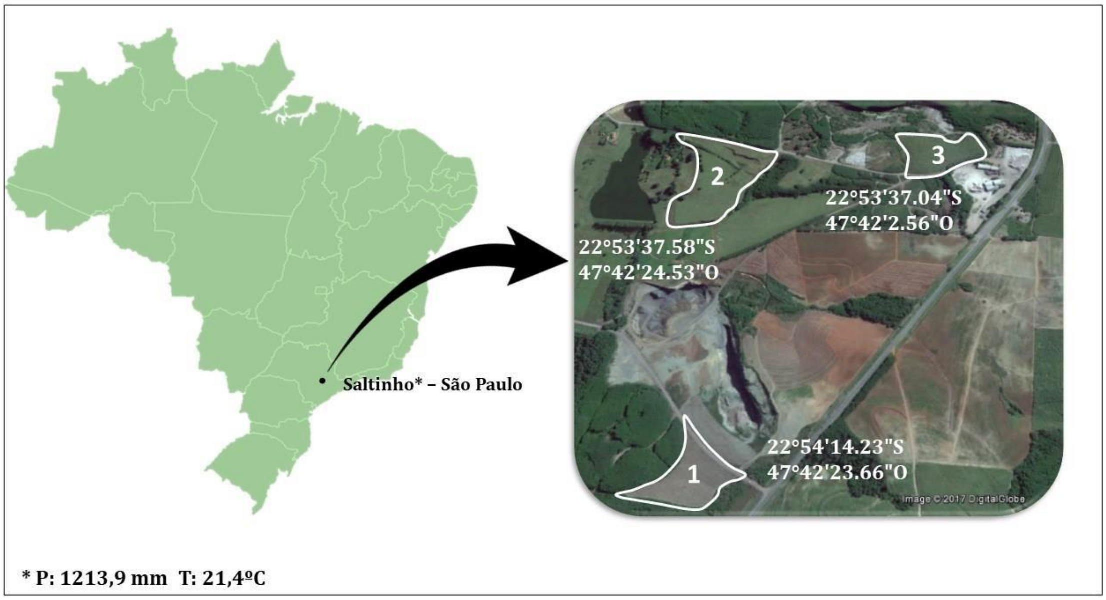

Fig. 1) Location of the study area: (1) Sugar-cane 2 years (SC2); (2) Sugar-cane 6 years (SC6) and (3) Pasture 20 years (P20). P: average annual rainfall, T: average annual temperature.

3.2.2. Soil sampling, exchangeable complex characterization and bulk chemical analysis

Soil samples were collected in the 0-5, 5-10 and 10-20 cm depths from the soil pits at SC2, SC6 and P20 sites to compose the bulk soil samples. Individual plants were collected and taken to laboratory for rhizosphere soil sampling. The rhizosphere soil samples were obtained following the method suggested by (Otero et al., 2012): only the soil firmly adhered to the roots, at a distance of approximately 0 to 2.0 mm from the root surface, was considered. After vigorous shaking of the roots, the detached soil was discarded. The soil material that remained adhered was brushed from roots. Rhizosphere soil samples were collected from 5 individual plants (in order to provide sufficient soil material for the analyzes) in the vicinity of the soil pits, in triplicate.

All samples were dried at 40º C for 72 h and passed through 2 mm and 0,025mm (for organic carbon determination) sieves before analysis. The pH was determined with a glass electrode in deionized water (soil: solution ratio, 1:2,5). Available P was extracted with Mehlich 1 solution and determined by spectrophotometry, whereas exchangeable Ca^{2+} and Mg^{2+} were extracted with KCl 1.0 mol L^{-1} solution and determined by atomic absorption spectroscopy (Perkin Elmer 1100B). Potential acidity (H+Al) was determined by titration of the solution with NaOH after extraction with calcium acetate at pH 7.0. X-ray fluorescence analyses were conducted using a portable XRF spectrometer (Olympus Delta DP-200) to determine the elemental composition of the samples.

3.2.3. Total organic carbon (TOC), dissolved organic carbon (DOC) and soil enzymes

Carbon content in soil samples were measured in a Soil Sample Combustion Unit (SSM-5000A) and the determination of TOC followed the methods described by Cambardella (2011). DOC was extracted from the rhizosphere with 10 mM NaH_2PO_4 (1 soil: 4 solution ratio), according to the method described in Mimmo et al. (2008) and the carbon content was measured in a TOC-LCSN/LCPN analyzer. Microbial status was evaluated by determining the enzymatic activity in the rhizosphere and bulk soil samples. Following the methods described Tabatai (1994) and Dick et al. (1996) acid phosphatase, β -glucosidase and arylsulfatase enzymes were determined by molecular absorption spectroscopy of the p-nitrophenol formed after the addition of the substrates specific to each enzyme.

3.2.4. Mineralogical analyses and weathering index

Clay fraction of the rhizosphere and bulk soils were investigated by X-ray diffraction (XRD). Samples were pretreated to remove organic matter with sodium hypochlorite (Anderson, 1961) and Fe oxides with dithionite-citrate-bicarbonate method (Mehra and Jackson, 1960). Sand was removed by wet sieving after dispersion of the suspension with 0.01mg L^{-1} Na_2CO_3 solution, and the clay fraction was separated from silt by sedimentation (Stoke's Law). XRD was performed on randomly dispersed powder for the silt fraction samples whereas the clay fraction was saturated with $MgCl_2$ and KCl at room temperature and with ethylene glycol, exposing the samples to the reagent at 60ºC for 20h. Thermal treatment at 550ºC was conducted as well for K-saturated samples. Thin films were deposited onto glass slides by pipetting a small amount of water dispersed sample and scanned from 3 to 35° 2θ, with 0.02° 2θ step size and 2s per step count time, using a Rigaku Miniflex II (CuKα radiation). Analysis by scanning electron microscopy (SEM) coupled with energy dispersion spectrometry (EDS) were performed on silt samples to investigate the patterns of alteration and degree of weathering of different primary minerals. The Ruxton ratio weathering index ($R = SiO_2/Al_2O_3$) was calculated to compare rhizosphere and bulk soil data.

3.2.5. Statistical analyses

The discriminant analysis (DA) was employed to contrast rhizosphere and bulk soil soil enzymes, chemical and XRF data, while a principal component analysis (PCA) was applied to rhizosphere and bulk soil from SC2, SC6 and P20 separately. Pearson correlation coefficients were used to assess the relationship between variables.

3.3. Results

Results from chemical, XRF and soil enzymes analyses are shown in Table 1. P20 exhibited the highest values of microbial activity, followed by SC6 and SC2. TOC, DOC and Ca were also higher in P20. SC2 presented the largest contents of phosphorus, followed by P20.

The discriminant analysis indicates that rhizosphere and bulk soil are contrasting biogeochemical environments. TOC, DOC, enzymatic activity, m%, SiO_2 and Al_2O_3 were higher in the rhizosphere, while pH decreased markedly. SiO_2 and Al_2O_3 contents are higher in the rhizosphere and the Ruxton ratio index indicates a greater concentration of silica relative to aluminum. The principal component analysis (Fig. 3) evidences that TOC, exchangeable Ca and microbial activity are correlated and that pH is inversely related to total silica, aluminum and iron contents. This analysis separated the P20 from SC2 and SC6, based on the higher TOC and enzymatic activity in this area (PC1 axis).

SEM-EDS data evidenced the higher degree of mineral weathering of silt minerals at the rhizosphere when compared to those from the bulk soil (Fig. 4 and 5). Quartz from P20 rhizosphere (Fig. 5a) exhibited etch pitting patterns on the crystal surface, not observable in the bulk soil (Fig. 4a). According to the criteria proposed by Read et al., (1996), feldspars from the bulk soil (Fig. 4d, e and f) showed little or no etching, clean surface and little or no alteration products (low/ medium low weathering class); conversely, these minerals showed an increased etch pitting, edges corrosion and coating secondary products (medium high weathering class) in the rhizosphere. Pyrite from the bulk soil (Fig. 4c) showed a preserved euhedral form which was lost in the rhizosphere where it appeared with rounded edges and covered by alteration products (Fig 5c). Talc and muscovite were more conserved in the bulk soil (Fig. 4b, g and h) while they presented an advanced pellicular pattern of weathering in the rhizosphere (Fig. 5b and h). Muscovite from SC2 rhizosphere (Fig 5g) shows a combination of pellicular and linear alteration pattern.

XRD investigation (Fig. 6) of clay evidenced kaolinite and illite in the bulk soil and in the rhizosphere of SC2. An illite peak at 1.0 nm was absent in both samples. SC6 samples, on the other hand, showed illite and kaolinite in the clay fraction from both rhizosphere and bulk soils. In the rhizosphere, however, the 1.0nm peak of illite appeared only in the samples treated with K. Lastly, P20 presented a different composition of clay fraction, containing smectite, illite and kaolinite. Again, the 1.75-1.80 nm peak after glycolation was evidenced only in the rhizosphere sample.

Table 1. Chemical, XRF, enzymatic activity results and Ruxton ratio index of rhizosphere and bulk soil from three studied areas

Sample	SC2		SC6		P20	
	Rhizosphere	Bulk	Rhizosphere	Bulk	Rhizosphere	Bulk
pH	6.20 ± 0.04	7.13 ± 0.12	5.50 ± 0.05	6.90 ± 0.10	6.70 ± 0.03	7.23 ± 0.06
TOC (%)	1.55 ± 0.15	0.60 ± 0.21	1.21 ± 0.35	0.65 ± 0.17	13,62 ± 2.23	9.27 ± 2.51
DOC (mg L^{-1})	32.46 ± 2.54	10.52 ±1.76	42.75 ± 6.80	14.82 ± 4.87	80.41 ± 25.28	56.78 ± 15.36
Ca (cmolc kg^{-1})	12.06 ± 0.18	9,92 ± 0.41	11.03 ± 0.16	10.91 ± 0.87	20.60 ± 1.06	16.90 ± 1.19
Mg (cmolc kg^{-1})	12.69 ± 0.16	12.22 ± 0.87	14.00 ± 0.13	12.22 ± 0.87	10.46 ± 0.19	14.95 ± 1.40
P (mg kg^{-1})	166.89 ± 41.32	125.30 ± 6.63	85.36± 7.52	19.22 ± 2.07	80.98 ± 11.53	41.56 ± 10.07
m%	0.12 ± 0.04	0.04 ± 0.01	5.17 ± 0.08	0.03 ± 0.02	0.45 ± 0.08	0.02 ± 0.01
SiO_2 (%)	39.14 ± 2.54	17.99 ± 0.94	45.12 ± 1.06	18.33 ± 0.92	28.79 ± 2.55	13.62 ± 1.53
Al_2O_3 (%)	13.54 ± 0.34	7.25 ± 0.40	15.23 ± 0.58	7.68 ± 1.30	6.77 ± 0.96	4.04 ± 0.25
Fe_2O_3 (%)	5.55 ± 0.17	4.53 ± 0.33	5.48 ± 0.05	4.60 ± 0.40	5.07 ± 0.53	5.65 ± 0.48
β -glucosidase (μg g^{-1} h^{-1})	56.04 ± 12.29	12.28 ± 1.07	122.53 ±26.44	24.59 ± 7.53	285.27 ± 64.85	56.95 ± 6.88
Arylsulfatase (μg g^{-1} h^{-1})	43.96 ± 24.02	43.32 ± 2.60	158.17 ± 39.38	51.69 ± 21.37	511.54 ± 145.35	148.85 ± 18.44
Acid Phosphatase (μg g^{-1} h^{-1})	427.37 ± 125.53	355.14 ± 9.78	527.10 ± 157.49	361.41 ± 22.77	638.10 ± 258.20	477.24 ± 6.09
Ruxton Ratio	2.89	2.48	2.96	2.39	4.25	3.37

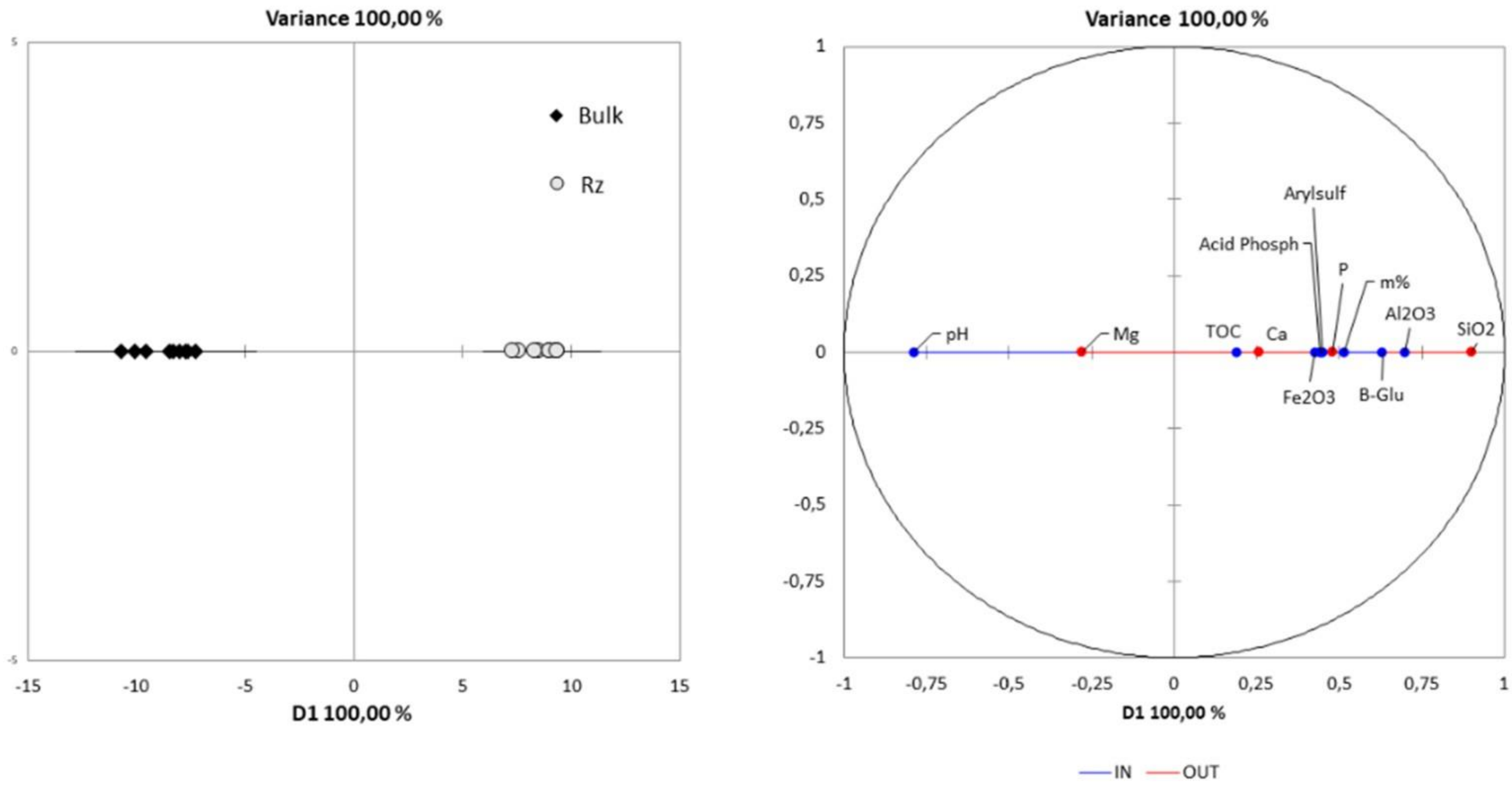

Fig. 2) Biplots of discriminant analysis of all rhizosphere and bulk soil samples from the three studied areas

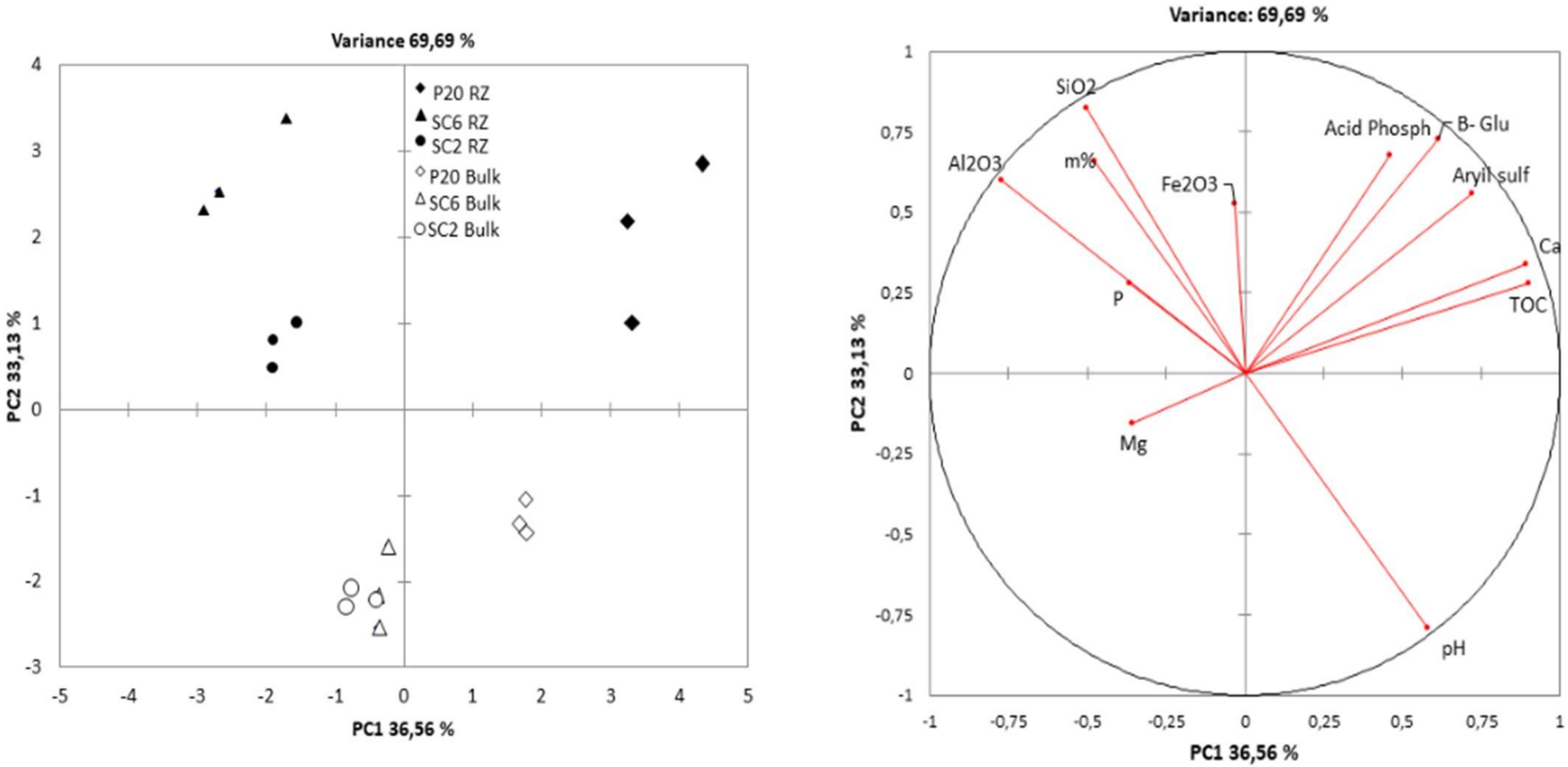

Fig. 3) Biplots of principal components analysis of rhizosphere and bulk soil samples from SC2, SC6 and P20, individually.

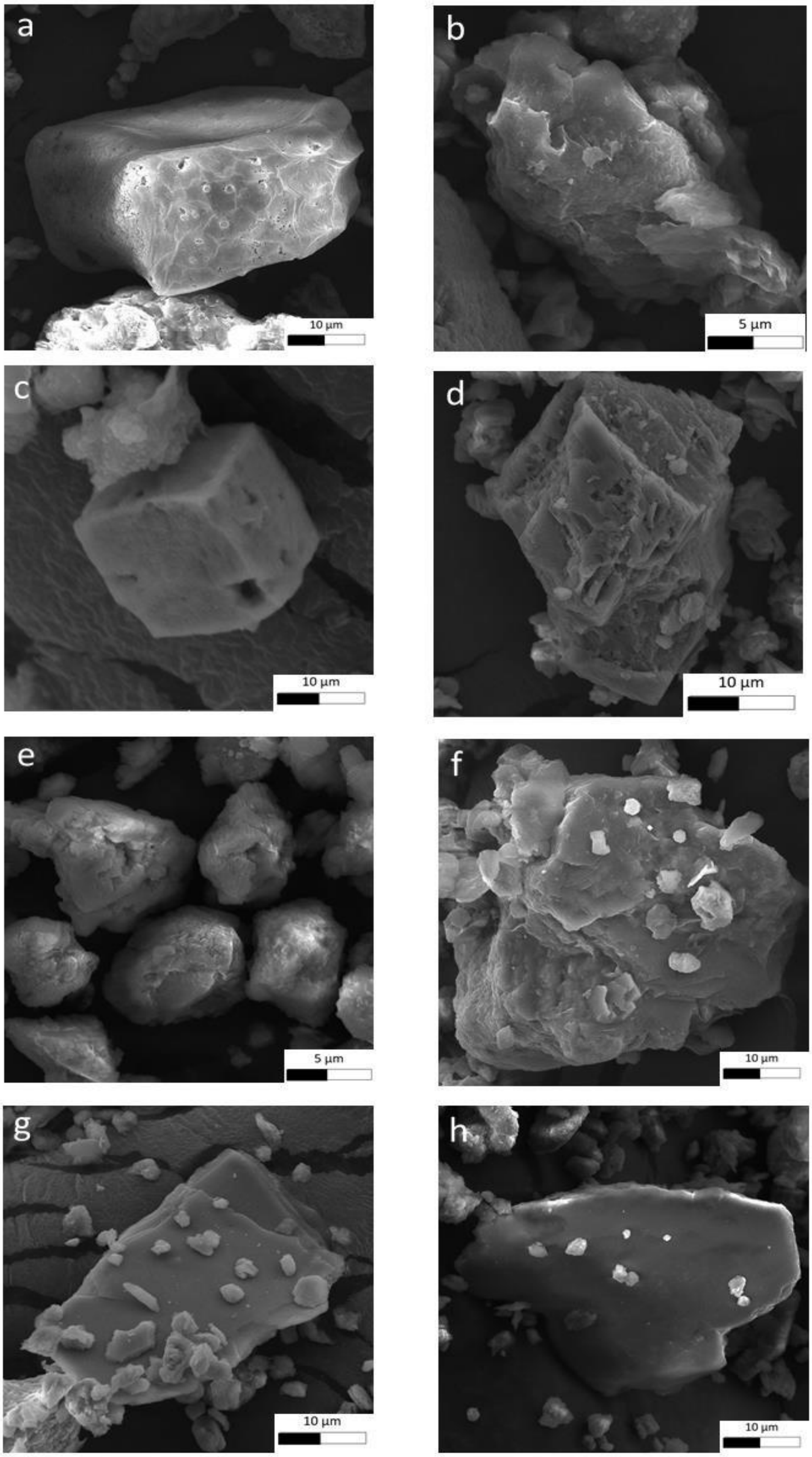

Fig. 4) MEV images from primary minerals in the bulk soil:(a) quartz from P20, (b) talc from P20, (c) pyrite from P20, (d) Na- feldspar from P20, (e) Na- feldspar from SC6, (f) Na-feldspar from SC2, (g) muscovite from SC2 and (h) muscovite from SC6.

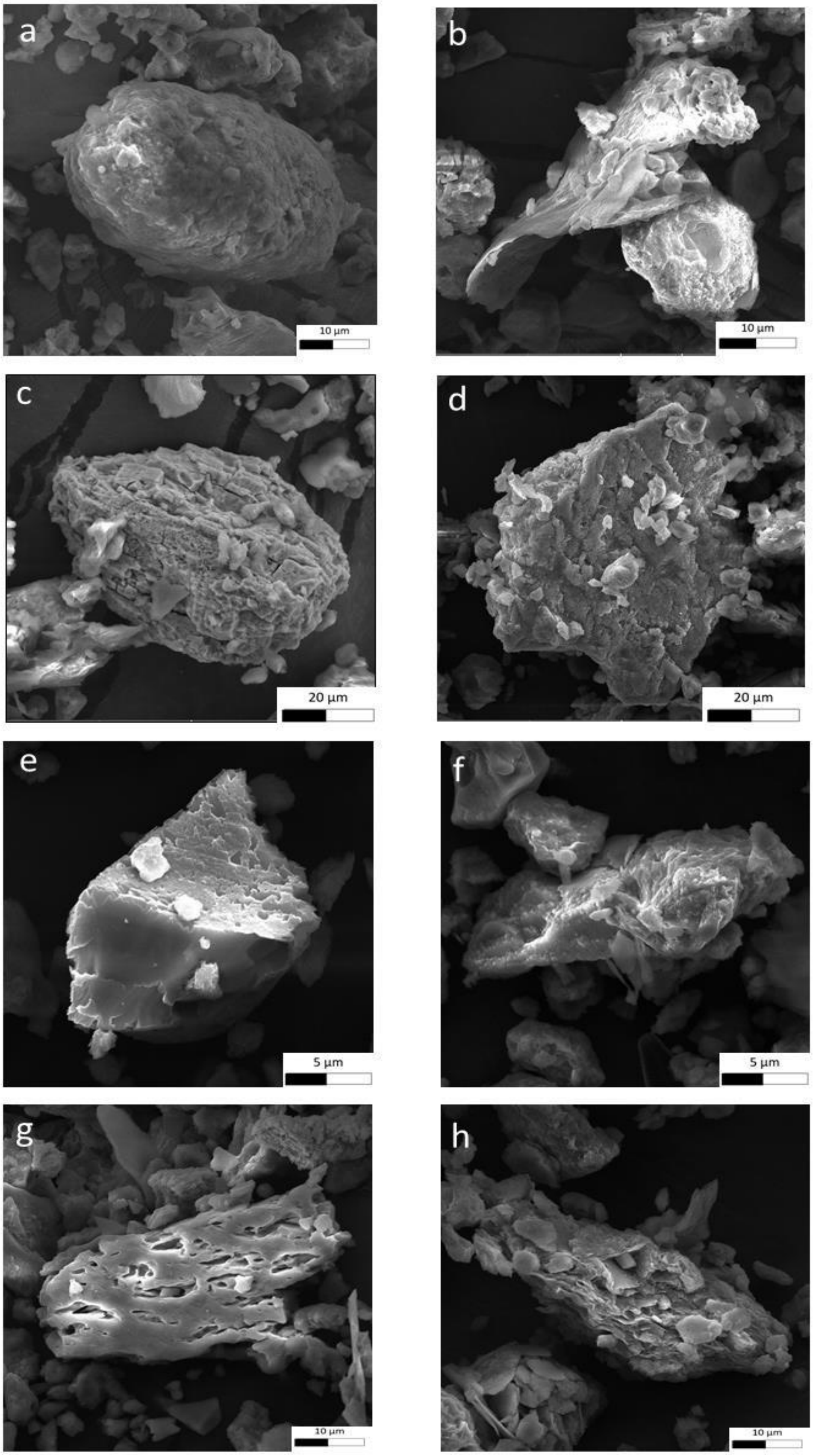

Fig. 5) MEV images from primary minerals from the rhizosphere: (a) quartz from P20, (b) talc from P20, (c) pyrite from P20, (d) Na- feldspar from P20, (e) Na- feldspar from SC6, (f) Na-feldspar from SC2, (g) muscovite from SC2 and (h) muscovite from SC6.

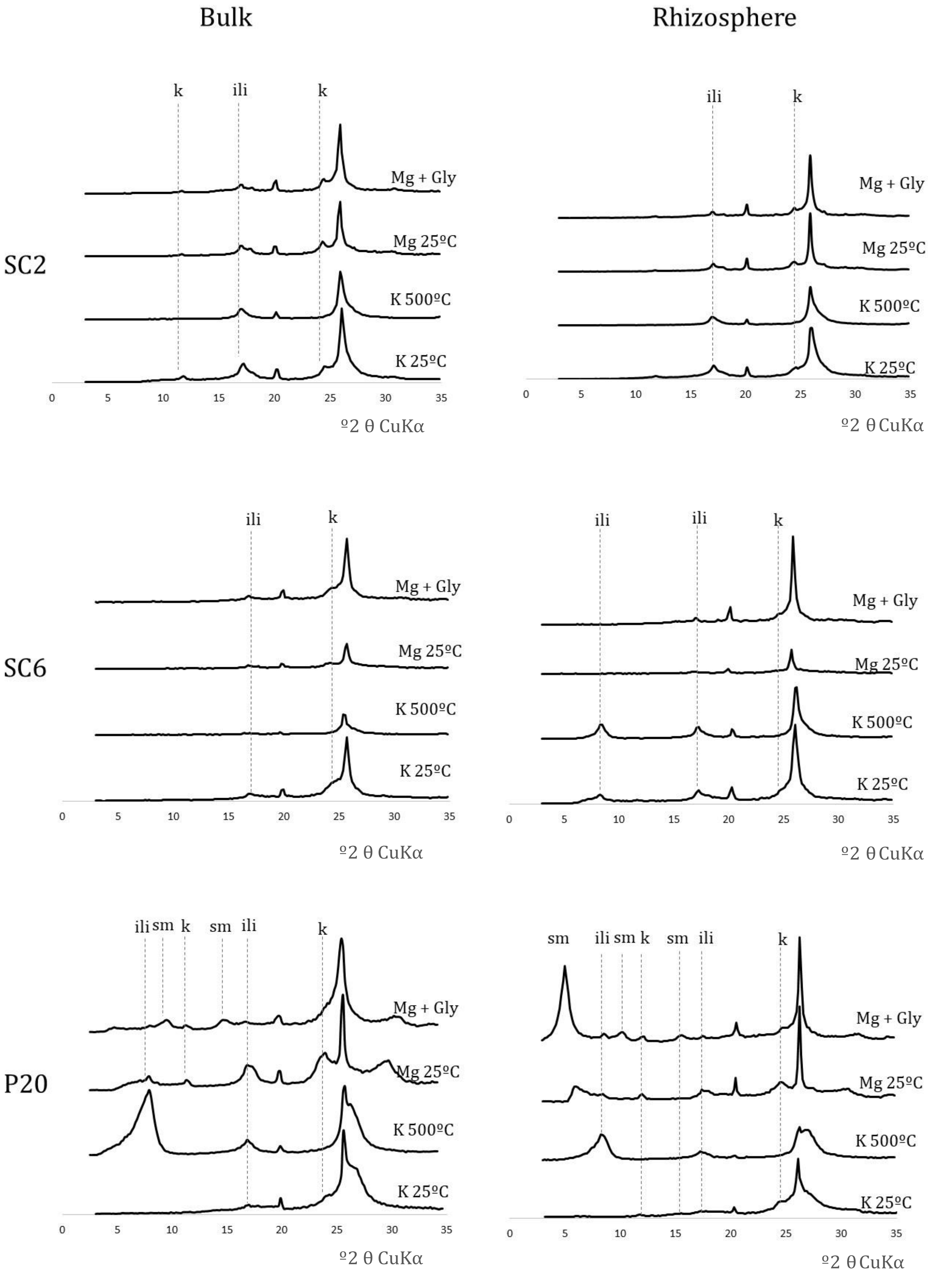

Fig. 6) XRD patterns from rhizosphere and bulk soil samples from SC2, SC6 and P20.

3.4. Discussion

SC2 presented the highest phosphorous concentration both in the bulk soil and the rhizosphere even though the acid phosphatase activity was the lowest. This suggests that, besides the mineralization of organic matter, there must be an inorganic source of P in this soil. As seen in Chapter 1, hydroxyapatite was found in P20, probably associated to black shales. Since SC2 and SC6 contain only few black shales fragments (artefacts), the probable source of inorganic P may have been depleted in SC6, explaining its low P contents.

Lower pH values, higher DOC contents and enzymatic activity indicate that the rhizosphere is creating conditions for mineral weathering mainly through acidification, exudation of organic chelating acids, and through the metabolism of their associated microorganisms (Boyle and Voigt, 1973; Mapelli et al., 2012).

The organic acids exuded by plants and those produced by microbial activity are affecting mineral weathering rates. The etch surfaces in the minerals under rhizosphere influence of the Technosols are a clear result of this process. Due to their high complexing ability, organic acids can solubilize Si and Al from the primary minerals crystal structure (Drever and Vance, 1994; Huang and Keller, 1970). Besides quartz high stability, previous work evidenced its dissolution byorganicacids (Bennett et al., 1988), enriching the soil solution with Si. The higher contents of Al in the rhizosphere reflected on the m% value, especially in SC6, and may be related to feldspar weathering. As shown by Welch and Ullman, 1996 many organic ligands preferably remove Al during plagioclase dissolution leaving a residual surface enriched in Si and releasing Al to the solution. In addition to feldspar weathering, the transformation of mica into other clay minerals may also be an important source of Al to the soil solution.

As regards muscovite, organic acids also increase its dissolution rates as more K is released from the interlayer (Song and Huang, 1988). The presented alteration, pellicular and linear combined, is typical of the replacement of micaceous by secondary minerals accompanied by an increase in the mineral volume (Delvigne, 1998)

Talc is usually found in soils developed from ultrabasic rock or through the weathering of serpentinite deposits (Allen and Hajek, 1989). Although rare, talc can be found in sedimentary rocks when contact metamorphism occurs and dolomite is metamorphized, which occurred in the Irati Formation (Anjos and Guimarães, 2008). A pattern of alteration similar to mica appeared for this mineral, probably due to its 2:1

structure (Zelazny and White, 1989).

Pyrite in the rhizosphere is more altered. As shown by (Kantar, 2016), Fe (II)-complexed with organicligands are oxidized more strongly than the free Fe(II) species. The development of iron oxides in the process of sulfide weathering was documented as initial pedogenic development of Technosols from pyrite mines (Uzarowicz and Skiba, 2011).

Although both total silica and aluminum contents were higher in the rhizosphere, there was a greater concentration of silica relative to aluminum in the rhizosphere, which may be a consequence of the weathered primary phyllosilicates enriched with Si due to the release of Al. Si may also concentrate in the rhizosphere as monosilicic acid (H_4SiO_4) due to the high uptake rate of this element by tropical grasses (de Melo et al., 2010). The absence of some of the peaks of 2:1 clay minerals in the bulk soil XRD patterns may suggest that these minerals have poor crystallinity. In contrast, 2:1 peak pattern in the rhizosphere (especially for smectite in P20) are sharper. Assuming that neoformation of secondary minerals or transformation is taking place, this situation seems to be favored in the rhizosphere. In fact, the transformation of mica into smectite and mixed-layer mica-smectite was documented in Technosols developed on pyrite-bearing schists (Uzarowicz et al., 2011). The rhizosphere contribution to these mineral transformations was not assessed, though.

It has been shown that microorganisms can actively concentrate relevant chemical species for mineral formation in localized microenvironments and accelerate clay formation by acting as nucleation points (Tuck et al., 2006). Thus, the elevated SiO_2, Al_2O_3 contents and Si/Al ratio and the high microbial activity in P20 rhizosphere make this environment prone to the formation of 2:1 clay.

3.5. Conclusions

Despite the early development stage of the studied Technosols, the rhizosphere created a favorable environment for microbial growth. Consequently, the more intense biological activity enhanced weathering and led to deeper dissolution of primary minerals in the rhizospheric environment. Further, the elevated microbial activity, the favorable geochemical conditions with high Si/Al ratio and the XRD patterns suggest the neoformation of 2:1 clay minerals and/or the transformation of primary to secondary minerals in the rhizosphere.

Mineral-biota interaction is a key factor on Technosol genesis. The chemical changes and mineral alterations promoted by the rhizosphere highlight the ability of plants and associated microorganisms to trigger soil formation. Thus, this study points to the importance of stimulating microbiota when aiming land reclamation, especially where the entire regolith was removed and pedogenesis re-starts from time zero.

References

Allen, B.L., Hajek, B.F., 1989. Mineral Occurrence in Soil Environments, in: Minerals in Soil Environments, SSSA Book Series SV - 1. Soil Science Society of America, Madison, WI, pp. 199–278. https://doi.org/10.2136/sssabookser1.2ed.c5

Anderson, J., 1961. An Improved Pretreatment for Mineralogical Analysis of Samples Containing Organic Matter1, Clays and Clay Minerals - CLAYS CLAY MINER. https://doi.org/10.1346/CCMN.1961.0100134

Anjos, C. W. D., Guimarães, E. M., 2008. Contact metamorphism in the Permian Irati Formation, north part of Paraná Basin (Brazil). Revista Brasileira de Geociências 38, 629-641.

Bennett, P.C., Melcer, M.E., Siegel, D.I., Hassett, J.P., 1988. The dissolution of quartz in dilute aqueous solutions of organic acids at 25°C. Geochim. Cosmochim. Acta 52,1521– 1530.https://doi.org/https://doi.org/10.1016/0016-7037(88)90222-0

Boyle, J.R., Voigt, G.K., 1973. Biological weathering of silicate minerals. Plant Soil 38, 191– 201. https://doi.org/10.1007/BF00011226

CEPAGRI - Centro de Pesquisas Meteorológicas e Climáticas Aplicadas à Agricultura. Climas dos municípios paulistas. Available on: http://www.cpa.unicamp.br/outras- informacoes/clima_muni_509.html>.

Dick, R.P., Breakwell, D.P., Turco, R.F., 1996. Soil enzymes activities and biodiversity measurements as integrative microbiological indicators. In: Doran, J.W.; & Jones, A.J.,eds. Methods for assessing soil quality. Soil Soc. Am.p. 247- 271. (Specialpublication, 49)

Drever, J.I., Vance, G.F., 1994. Role of Soil Organic Acids in Mineral Weathering Processes BT - Organic Acids in Geological Processes, in: Pittman, E.D., Lewan, M.D. (Eds.), . Springer Berlin Heidelberg, Berlin, Heidelberg, pp. 138–161. https://doi.org/10.1007/978-3-642-78356-2_6

Crowley, E. D., 2006. Microbial Siderophores in the Plant Rhizosphere, Iron Nutrition in Plants and Rhizospheric Microorganisms. https://doi.org/10.1007/1-4020-4743- 6_8

Egamberdieva, D., Wirth, S.J., Alqarawi, A.A., Abd_Allah, E.F., Hashem, A., 2017. Phytohormones and Beneficial Microbes: Essential Components for Plants to

Balance Stress and Fitness. Front. Microbiol.

Garbeva, P., van Elsas, J., A. van Veen, J., 2008. Rhizosphere Microbial Community and Its Response to Plant Species and Soil History, Plant and Soil. https://doi.org/10.1007/s11104-007-9432-0

Gaskins, M.H., Albrecht, S.L., Hubbell, D.H., 1985. Rhizosphere bacteria and their use to increase plant productivity: A review. Agric. Ecosyst. Environ. 12, 99 –116. https://doi.org/https://doi.org/10.1016/0167-8809(85)90071-4

Hartmann, A., Rothballer, M., Schmid, M., 2008. Lorenz Hiltner, a pioneer in rhizosphere microbial ecology and soil bacteriology research, Plant Soil. https://doi.org/10.1007/s11104-007-9514-z

Huang, W.H., Keller, W.D., 1970. Dissolution of rock-forming silicate minerals in organic acids: Simulated first-stage weathering of fresh mineral surfaces. Am. Mineral. 55, 2076–2094.

Huot, H., Simonnot, M.-O., Morel, J.L., 2015. Pedogenetic Trends in Soils Formed in technogenic Parent Materials. Soil Sci. 180, 1. https://doi.org

IBGE, 2012. Brazilian Institute of Geography and Statistics. Technical Handbo ok of the Brazilian Vegetation, (second ed.), Rio de Janeiro, ISSN 0103-9598

Jongmans, A.G., van Breemen, N., Lundström, U., van Hees, P.A.W., Finlay, R.D., Srinivasan, M., Unestam, T., Giesler, R., Melkerud, P.-A., Olsson, M., 1997. Rock-eating fungi. Nature 389, 682.

Kantar, C., 2016. Role of low molecular weight organic acids on pyrite dissolution in aqueous systems: Implications for catalytic chromium (VI) treatment, Water Science and Technology. https://doi.org/10.2166/wst.2016.182

Leguédois, S., Séré, G., Auclerc, A., Cortet, J., Huot, H., Ouvrard, S., Watteau, F., Schwartz, C., Morel, J.L., 2016. Modelling pedogenesis of Technosols. Geoderma 262, 199 –212. https://doi.org/10.1016/j.geoderma.2015.08.008

Lucas, Y., 2001. The Role of Plants in Controlling Rates and Products of Weathering: Importance of Biological Pumping. Annu. Rev. Earth Planet. Sci. 29, 135 –163. https://doi.org/10.1146/annurev.earth.29.1.135

Mapelli, F., Marasco, R., Balloi, A., Rolli, E., Cappitelli, F., Daffonchio, D., Borin, S., 2012. Mineral-microbe interactions: Biotechnological potential of bioweathering. J. Biotechnol. 157, 473–481. https://doi.org/10.1016/j.jbiotec.2011.11.013

Mehra, P., Jackson, M. O., L., 1960. Iron Oxide Removal From Soils and Clays by Dithionite- Citrate Systems Buffered With Sodium Bicarbonate, Clays and Clay Minerals. https://doi.org/10.1346/CCMN.1958.0070122

Melo, S.P., Monteiro, F.A., De Bona, F.D., 2010. Silicon distribution and accumulation in shoot tissue of the tropical forage grass Brachiaria brizantha. Plant Soil 336, 241 –249. https://doi.org/10.1007/s11104-010-0472-5

Mimmo, T., Ghizzi, M., Marzadori, C., Gessa, C.E., 2008. Organic acid extraction from rhizosphere soil : effect of field-moist , dried and frozen samples 175–184. https://doi.org/10.1007/s11104-008-9574-8

Nannipieri, P., Ascher-Jenull, J., Ceccherini, M.T., Landi, L., Pietramellara, G., Renella, G., Valori, F., 2008. Effects of Root Exudates in Microbial Diversity and Activity in Rhizosphere Soils, Molecular Mechanisms of Plant and Microbe Coexistence. https://doi.org/10.1007/978-3-540-75575-3_14

Otero, X.L., Álvarez, E., Fernández-Sanjurjo, M.J., Macías, F., 2012. Micronutrients and toxic trace metals in the bulk and rhizospheric soil of the spontaneous vegetation at an abandoned copper mine in Galicia (NW Spain). J. Geochemical Explor.112,8492.https://doi.org/https://doi.org/10.1016/j.gexplo.2011.07.007

Read, G., Kemp, R.A., Rose, J., 1996. Development of a feldspar weathering index and its application to a buried soil chronosequence in southeastern England. Geoderma 74, 267–280. https://doi.org/https://doi.org/10.1016/S0016-7061(96)00069-9

Song, S.K., Huang, P.M., 1988. Dynamics of Potassium Release from Potassium-Bearing Minerals as Influenced by Oxalic and Citric Acids. Soil Sci. Soc. Am. J. 52, 383–390. https://doi.org/10.2136/sssaj1988.03615995005200020015x

TABATABAI, M.A. 1994. Soil enzymes. In: WEAVER, R.W.; SCOTT, A. & BOTTOMELEY, P.J., eds. Methods of soil analysis: microbiological and biochemical properties.Madison,Soil Sci. Soc. Am., 2:778-835,. (Special Publication, 5)

Tosca, N.J., Macdonald, F.A., Strauss, J. V, Johnston, D.T., Knoll, A.H., 2011. Sedimentary talc in Neoproterozoic carbonate successions. Earth Planet. Sci. Lett. 306, 11–22. https://doi.org/https://doi.org/10.1016/j.epsl.2011.03.041

Tuck, V.A., Edyvean, R.G.J., West, J.M., Bateman, K., Coombs, P., Milodowski, A.E., McKervey, J.A., 2006. Biologically induced clay formation in subsurface granitic environments. J. Geochemical Explor. 90, 123–133. https://doi.org/https://doi.org/10.1016/j.gexplo.2005.09.007

Uteau, D., Hafner, S., Kouso Pagenkemper, S., Peth, S., Wiesenberg, G., Kuzyakov, Y., Horn, R., 2015. Oxygen and redox potential gradients in the rhizosphere of alfalfa grown on a loamy soil, Journal of Plant Nutrition and Soil Science. https://doi.org/10.1002/jpln.201300624

Uzarowicz, Ł., Skiba, S., 2011. Technogenic soils developed on mine spoils containing iron sulphides: Mineral transformations as an indicator of pedogenesis. Geoderma 163, 95–108. https://doi.org/https://doi.org/10.1016/j.geoderma.2011.04.008

Uzarowicz, Ł., Skiba, S., Skiba, M., Segvic, B., 2011. Clay-mineral Formation in Soils Developed in the Weathering Zone of Pyrite-Bearing Schists: A Case Study from the Abandoned Pyrite Mine in Wieściszowice, Lower Silesia, SW Poland, Clays and Clay Minerals. https://doi.org/10.1346/CCMN.2011.0590604

Welch, S.A., Ullman, W.J., 1996. Feldspar dissolution in acidic and organic solutions: Compositional and pH dependence of dissolution rate. Geochim. Cosmochim. Acta 60, 2939–2948. https://doi.org/https://doi.org/10.1016/0016-7037(96)00134-2

Welch, S.A., Ullman, W.J., 1993. The effect of organic acids on plagioclase dissolution rates and stoichiometry. Geochim. Cosmochim. Acta 57, 2725–2736. https://doi.org/https://doi.org/10.1016/0016-7037(93)90386-B

Zelazny, L.W., White, G.N., 1989. The Pyrophyllite-Talc Group, in: Minerals in Soil Environments, SSSA Book Series SV - 1. Soil Science Society of America, Madison, WI, pp. 527–550. https://doi.org/10.2136/sssabookser1.2ed.c11

4. FINAL CONSIDERATIONS

The present study highlights that constructed tropical soils may evolve in an accelerated rate of pedogenesis and, thus, are a real alternative for the reclamation of severely degraded areas where natural soils were completely lost. Although soil degradation resulting from mining activities occur really fast, in particular cases where mine wastes are free from pollutants, simple techniques as fulfilling the former pits with the mine spoils can lead to positive outcomes, e.g. food and energy production. The combination of grasses over Ca-rich mine spoils may trigger high organic carbon stocks, even surpassing the contents found in the surrounding natural soils.

The role of organisms in the pedogenesis of such incipient soils is paramount. Chapter 2 shows that weathering is highly pronounced in the rhizosphere of these constructed Technosols where soil organisms significantly fuel pedogenesis. Therefore, the reclamation strategies for degraded areas should aim to stimulate soil biota, from the macro to the micro scales accelerating soil formation in constructed soils and, thus, increasing the success of the revegetation programs.

This study evidences the need for more research on Technosols in the tropical environment and also consists in a pioneer contribution to the incorporation of Technosol into the Brazilian system of soil classification (SiBCS). To gather more information about the real potential of these soils on land reclamation, future studies should focus on elucidating the real ability of Technosols to provide ecosystem services.

ANNEXES

Annex A. Extra information of the sugar cane 2 years area (SC2)

Fig A1) Rehabilitated area cultivated with sugar-cane for 2 years (SC2) in July 2017.

Fig A2) SC2 in February 2018.

Fig A3) Soil profile from SC2: Hyperskeletic Spolic Technosol (Clayic)

Soil description of SC2 profile

Hyperskeletic Spolic Technosol (Clayic)

Location: Saltinho (SE- Brazil, State of São Paulo)

Coordinates: 22°54'14.23"S, 47°42'23.66"O

Soil moisture and temperature regime: Udic isohyperthermic

Relief: Plain

Land use: sugar cane crop grown on rehabilitated open cast limestone mine

Parent material: technogenic redeposited natural material (limestone mine spoils)

Description:

Au (0-7cm): silty clay, dark grayish brown (10YR 4/2), few reddish yellow (7.5 YR 6/8) mottles, weak fine granular structure, very friable, slightly sticky, plastic; abundant coarse siltstone fragments (25% coarse, 30% medium, 35% fine gravel) and; common fine roots; clear smooth boundary

Cu1 (7-20cm): silty clay, dark gray (10YR 4/1), few reddish yellow (7.5 YR 6/8) mottles, very weak veryfine granular and single grain structure, very friable, slightly sticky, plastic, abundant coarse siltstone fragments (30% stones 25% coarse, 20% medium, 15% fine gravel), and very few black shale fragments (medium and fine gravel); few fine roots, clear smooth boundary

Cu2 (20-33cm): silty clay, dark gray (10YR 4/1), few reddish yellow (7.5 YR 6/8) single grain structure, slightly sticky, plastic; dominant and very loose coarse siltstone fragments (50% coarse, 30% medium, 20% fine gravel) and very few black shale fragments; very few fine roots, clear smooth boundary.

Cu3 (33-52cm): silty clay, dark gray (10YR 4/1), few reddish yellow (7.5 YR 6/8) mottles, single grain structure, slightly sticky, plastic; dominant and very loose coarse siltstone fragments, (40% stones 25% coarse, 10% medium, 15% fine gravel) and very few black shales fragments; very few fine roots, clear smooth boundary.

Cu4 (52-70+): silty clay, dark gray (10YR 4/1), weak very fine granular structure, very friable, slightly sticky, plastic; dominant and very loose coarse siltstone fragments (40% coarse, 40% medium, 20% fine gravel) and very few black shale fragments; very few fine roots.

Annex B. Extra information of the sugar cane 6 years area (SC6)

Fig. A4) Sugar cane growing for 6 years in a former open cast rehabilitated (SC6).

Fig. A5) Former limestone quarry at SC6.

Fig A6) Soil profile from SC6: Hyperskeletic Spolic Technosol (Clayic, Endoraptic).

Soil description of SC6 profile

Hyperskeletic Spolic Technosol (Clayic, Endoraptic)

Soil moisture and temperature regime: Udic isohyperthermic

Relief: Plain

Land use: sugar cane crop grown on rehabilitated open cast limestone mine Parent

material: technogenic redeposited natural material (limestone mine spoils)

Au (0-9cm): clay, dark grayish brown (10YR 4/2), abundant reddish yellow (7.5 YR 6/8) mottles and common fine red (2.5 YR 4/8), weak to moderate medium granular structure, friable, sticky, plastic; abundant coarse siltstone and few coarse black shale fragments, 10% coarse gravel, 35% medium gravel, 30% fine gravel; common fine roots; clear smooth boundary

CAu (11-21cm): clay, dark gray (10YR 4/1), abundant reddish yellow (7.5 YR 6/6), common red (2.5 YR 4/8) and few black (10YR 2/1), mottles, weak fine granular and single grain structure, friable, sticky, plastic; abundant coarse siltstone and few coarse black shale fragments, 20% coarse gravel, 40% medium gravel, 20% fine gravel; few fine roots; clear smooth boundary.

Cu1 (21-35cm): clay, dark gray (10YR 4/1), common reddish yellow (7.5 YR 6/6) and few red (2.5 YR 4/8) mottles, weak fine granular and single grain structure, very friable, sticky, plastic; dominant and very loose siltstones and common black shale fragments, 50% stones, 20% coarse, 10% medium, 10% fine gravel; few fine roots; clear smooth boundary.

Cgu2 (35-52 cm): silty clay, reddish yellow (7.5 YR 6/8), many darkgray (10YR 4/1), and very few red (2.5 YR 4/8) mottles, weak fine granular and weak medium blocky subangular structure, friable, sticky, plastic; many siltstones and few black shale fragments, 55% medium and 30% fine gravel, abrupt smooth boundary.

2Chu3 (52-60cm+): sandy clay loam, very dark gray (10YR 3/1), few reddish yellow (7.5 YR 6/8) mottles, weak fine granular structure, friable, slightly sticky, slightly plastic; abundant black shale fragments, 20% coarse, 40% medium, 20% fine gravel; few fine roots; petrochemical odor.

Black shale layer (60cm+).

Annex C. Extra information of the pasture area (P20)

Fig A7) Rehabilitated area where pasture is cultivated for 20 years (P20).

Fig A8) Former limestone quarry from P20 area.

Fig A9) Soil profile from P20: Hyperskeletic Spolic Technosol (Hyperhumic, Loamic, Somerimollic).

Soil description of P20 profile

Hyperskeletic Spolic Technosol (Hyperhumic, Loamic, Somerimollic) Soil moisture and temperature regime: Udic isohyperthermic

Relief: Plain

Land use: pasture grown on rehabilitated open cast limestone mine

Parent material: technogenic redeposited natural material (limestone mine spoils)

Description:

Au1 (0-5 cm): loam, very dark brown (7.5 YR 2.5/2), strong medium and coarse crumb structure and moderate medium blocky subangular structure, firm, slightly sticky, slightly plastic; abundant coarse black shale, few coarse siltstones fragments and very few coarse dolomites; many fine and medium roots; clear smooth boundary;

Au2 (5-11 cm): loam, very dark brown (7.5 YR 2.5/2), moderate to strong medium granular crumb and moderate fine to medium blocky subangular structure, firm, slightly sticky, slightly plastic; abundant coarse black shale, few coarse siltstones fragments and very few coarse dolomites; many fine and medium roots; clear smooth boundary;

ACu (11-29cm): sandy clay loam, very dark brown (7.5 YR 2.5/2), moderate fine to medium granular structure, friable, slightly sticky, slightly plastic; abundant coarse black shale, few coarse siltstones fragments and very few coarse dolomites; many fine and medium roots; gradual smooth boundary;

ACu2 (29-60cm): sandy clay loam, very dark brown (7.5 YR 2.5/2), moderate fine granular structure, friable, slightly sticky, slightly plastic; dominant coarse black shale, few coarse siltstones fragments and very few coarse dolomites; common fine roots

Annex D. Details from the soil profiles

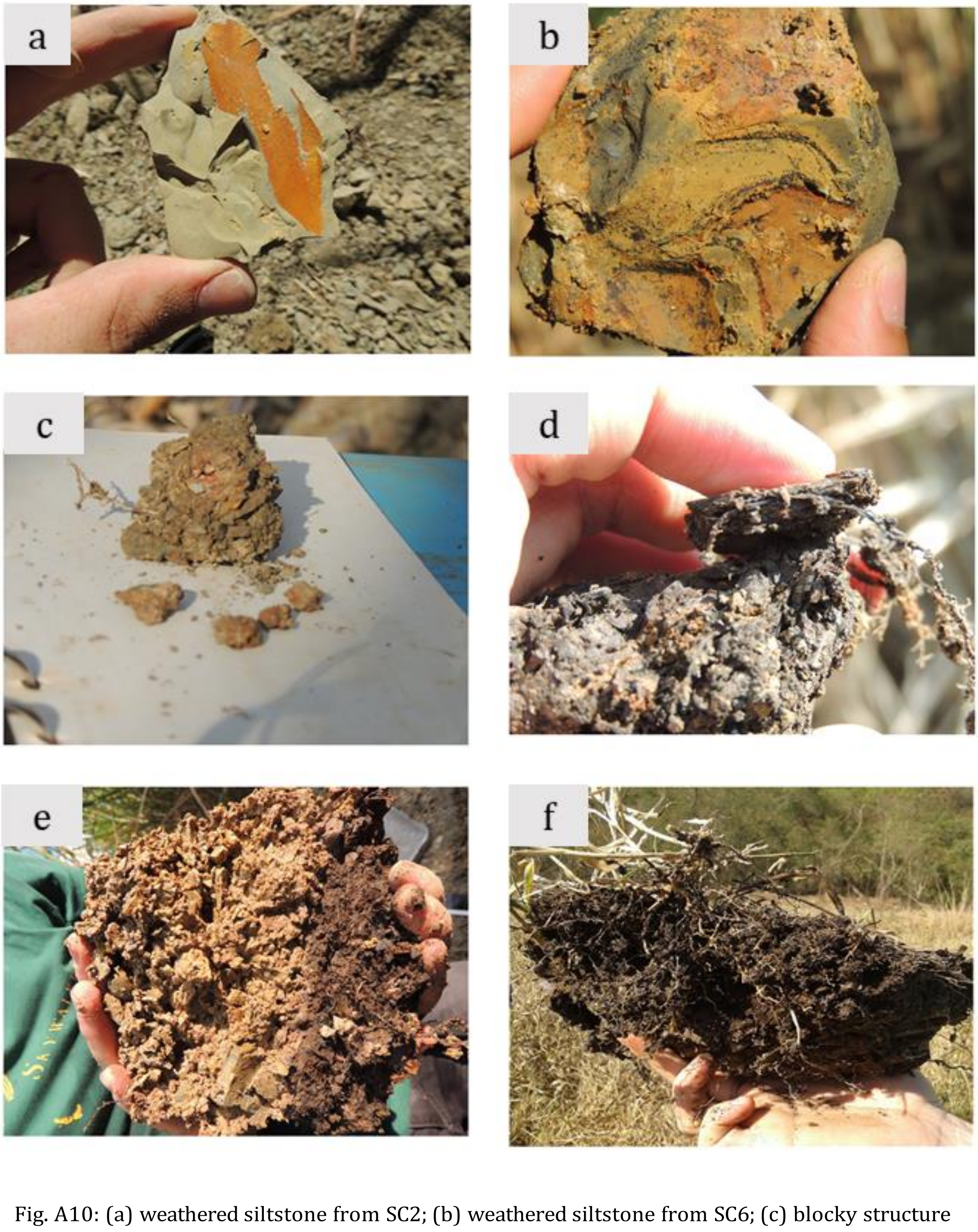

Fig. A10: (a) weathered siltstone from SC2; (b) weathered siltstone from SC6; (c) blocky structure in Cgu2 horizon from SC6; (d) roots penetrating a weathered black shale in 2Chu3 horizon from SC6; (e) abrupt boundary from Cgu2 to 2Chu3 (SC6); (f) crumb structure maintained by roots of *Brachiaria spp* in P20.